NASA CONTRACTOR REPORT

NASA CR-1748

PRINCIPLES FOR THE DESIGN OF ADVANCED FLIGHT DIRECTOR SYSTEMS BASED ON THE THEORY OF MANUAL CONTROL DISPLAYS

by D. H. Weir, R. H. Klein, and D. T. McRuer

Prepared by
SYSTEMS TECHNOLOGY, INC.
Hawthorne, Calif.
for Ames Research Center

NATIONAL AERONAUTICS AND SPACE ADMINISTRATION • WASHINGTON, D. C. • MARCH 1971

1. Report No.	2. Government Accession No.	3. Recipient's Catalog No.
NASA CR-1748		

4. Title and Subtitle	5. Report Date
Principles for the Design of Advanced Flight Director Systems Based on the Theory of Manual Control Displays	March 1971
	6. Performing Organization Code
7. Author(s)	8. Performing Organization Report No.
D. H. Weir, R. H. Klein and D. T. McRuer	
	10. Work Unit No.
9. Performing Organization Name and Address	
Systems Technology, Inc. Hawthorne, California	11. Contract or Grant No.
	NAS 2-3746
	13. Type of Report and Period Covered
12. Sponsoring Agency Name and Address	
National Aeronautics & Space Administration Washington, D.C. 20546	14. Sponsoring Agency Code

15. Supplementary Notes

16. Abstract

Recent developments in the theory of manual control displays lead to principles for analytical design of flight directors, given the dynamics of the (augmented) vehicle and its manual control system. The theory shows that there are effective director/vehicle controlled element dynamics which are preferred from the standpoint of pilot response and system performance. Other considerations include response compatibility, display consistency, and autopilot monitoring. This leads to rules and analytical procedures which allow the director computer feedbacks to be selected, weighted, and equalized to provide an effective director/vehicle system which satisfies both pilot-centered and guidance and control requirements. This report details and illustrates the analytical process for longitudinal control of transport-type aircraft during landing approach.

17. Key Words (Suggested by Author(s))	18. Distribution Statement
Flight Director Director Display Command Manual Control	UNCLASSIFIED-UNLIMITED

19. Security Classif. (of this report)	20. Security Classif. (of this page)	21. No. of Pages	22. Price*
UNCLASSIFIED	UNCLASSIFIED	99	$3.00

*For sale by the National Technical Information Service, Springfield, Virginia 22151

FOREWORD

The analytical design principles presented in this report represent an application of models and methods for the analysis and synthesis of manual control displays which were developed as part of an overall program in the manual control displays area. This applied research was conducted for the Man-Machine Integration Branch of the NASA Ames Research Center under Contract NAS2-3746. The NASA project monitors were M. K. Sadoff and W. D. Chase. The STI Technical Director was D. T. McRuer, and the project engineer for this part of the program was D. H. Weir.

The authors would like to thank those in the flight director industry who contributed data, ideas, and helpful suggestions during the course of this project. This includes Messrs. Roger Bishop of Smiths Industries Ltd.; K. E. Duning of Collins Radio Co.; Harry Miller of Sperry Rand Corp.; G. E. Ewalt of Lear-Siegler, Inc.; Harrison Wood of Bendix Corp.; Christopher Lewis of Elliott Brothers Ltd.; Arthur Barnes of British Aircraft Corp., Ltd.; and J. M. Naish of McDonnell-Douglas Corp.

Finally, we are particularly indebted to the STI Publications Department for their careful work in preparing the final manuscript.

ABSTRACT

Recent developments in the theory of manual control displays now make it feasible to state principles for a priori analytical design of a flight director, given the available sensed feedbacks and the dynamics of the vehicle and its manual control system. The principal result from the theory is that there are effective controlled element dynamics which are preferred from the standpoint of pilot response and system performance. Other considerations include response compatibility, display consistency, and autopilot monitoring. This leads to rules and analytical procedures which allow the feedbacks to be selected, weighted, and equalized to provide an effective flight director-plus-vehicle controlled element which is best for both pilot control and overall performance. This report details and illustrates this process for longitudinal control of transport-type aircraft during landing approach.

The flight director design requirements are determined in part by the guidance, control, and regulation demands of the pilot-vehicle closed-loop system in a given task. In addition, there are manual control requirements which help prescribe the equalization and relative weightings of the selected feedbacks whose sum gives the flight director command signal. In the process of satisfying the derived requirements, the analytical approach serves to:

- Isolate the effect of each feedback and show how it relates to the requirements.
- Determine the sensing and equalization on the feedbacks.
- Identify the practical compromises that must be made, as well as their effects.
- Suggest aerodynamic and other modifications to the vehicle which could improve the pilot-controlled system.

A manual control loop structure of altitude with elevator, and speed with throttle is used to illustrate the analyses. Conventional aircraft dynamics are assumed in which short-period-to-phugoid frequency ratio, static stability, and the low frequency zero in the altitude numerator are of key importance. The influence of direct lift control (DLC) and auto-throttles is also considered.

CONTENTS

FIGURES

TABLES

SYMBOLS

a_z	Vertical acceleration from 1g, positive down
A	Coefficient of highest order term in a transfer function
c	Mean aerodynamic chord
c.g.	Center of gravity
d	Deviation from glide slope beam, positive up
DLC	Direct lift control
FD	Flight director command bar motion
g	Gravity
G_b^a	Transfer function or describing function relating output, a, to input, b
h	Altitude perturbation about the initial x axis, positive up
ILS	Instrument Landing System
I_y	Moment of inertia about pitch axis
K	Linear gain
ℓ_x	Distance from c.g. to a longitudinal body station
m	Mass
M_q	$\frac{\rho S U_o c^2}{4 I_y} C_{M_q}$
M_u	$\frac{\rho S U_o c}{I_y} (C_M + C_{M_u})$
M_w	$\frac{\rho S U_o c}{2 I_y} C_{M_\alpha}$
$M_{\dot{w}}$	$\frac{\rho S c^2}{4 I_y} C_{M_{\dot{\alpha}}}$
M_δ	$\frac{\rho S U_o c}{2 I_y} C_{M_\delta}$
n_b	Beam noise
n_r	Glide slope receiver noise

$N_i^{\lambda}(s)$	Numerator of transfer function relating output, λ, to input, i
$N_{i_1 i_2}^{\lambda_1 \lambda_2}(s)$	Coupling numerator relating outputs, λ, to inputs, i
q	Pitch rate or dynamic pressure
R	Range
s	Laplace operator, $\sigma \pm j\omega$
S	Wing area
t	Time
$1/T$	Inverse time constant
u	Forward speed perturbation along x axis, positive forward
u_g	Gust along the aircraft's body-fixed x axis (tailwind positive)
U_o	Steady-state velocity along x_o axis
V_T	Total velocity
w	Vertical speed perturbation along z axis, positive down
w_g	Gust along the aircraft's body-fixed z axis (downdraft positive)
W	Weight
x	Perturbed longitudinal body-fixed stability axis
X_u	$\frac{\rho S U_o}{m}(-C_D - C_{D_u}) = -\frac{2g}{U_o}$
X_w	$\frac{\rho S U_o}{2m}(C_L - C_{D_\alpha})$
X_δ	$\frac{\rho S U_o^2}{2m}(-C_{D_\delta})$
z	Perturbed vertical body-fixed stability axis
Z_u	$\frac{\rho S U_o}{m}(-C_L - C_{L_u})$
Z_w	$\frac{\rho S U_o}{2m}(-C_{L_\alpha} - C_D)$
Z_δ	$\frac{\rho S U_o}{2m}(-C_{L_\delta})$

α	Angle of attack
γ	Flight path angle relative to initial x axis positive when rate of descent is decreased
δ	Control deflection, specialized by subscript
$\Delta(s)$	Denominator of airframe transfer function
ζ	Damping ratio
$\eta(s)$	General form for gust input
θ	Attitude perturbation from initial condition, positive nose up
Θ_o	Initial inclination of X_o axis, positive above horizon
ρ	Density
σ	Real portion of the complex variable s
ω	Angular frequency

Special Subscripts

c	Command
e	Error, or elevator control (positive TED)
f	Flap
g	Gust
GSR	Glide slope receiver
n	Natural
o	Initial value
p	Phugoid
sp	Short period
ss	Steady state
T	Throttle control
WO	Washout

SECTION I

INTRODUCTION

A. OBJECTIVE

The purpose of this report is to apply the existing "theory of manual control displays" to develop design principles for advanced flight director systems and to illustrate these principles in an example with a modern commercial transport.

The evolved design principles are applicable in general to the following control tasks:

- Landing approach
- Altitude hold
- Attitude hold

The emphasis in the analytical development and numerical example is on landing approach, from beam acquisition to flare initiation. This concentration on the ILS-guided landing task permits coverage of one of the most complex conditions for which flight directors are useful.

The flare maneuver is not included per se; however, a direct extension of the landing approach laws can be used to accomplish the flare. Similarly, with some minor modifications an attitude hold configuration could provide for takeoff rotation or initiation of go-around.

B. BACKGROUND

A flight director system combines display and computation elements with the pilot and effective (augmented) vehicle in a feedback control system. This combination is shown in Fig. 1 for the approach mode of operation. The flight director display presents both command and status information. The command elements provide lateral and vertical steering signals made up of a combination of desired path and aircraft motion quantities. These are shaped, filtered and mixed appropriately to permit the pilot to close the flight director system loop with ease and efficiency.

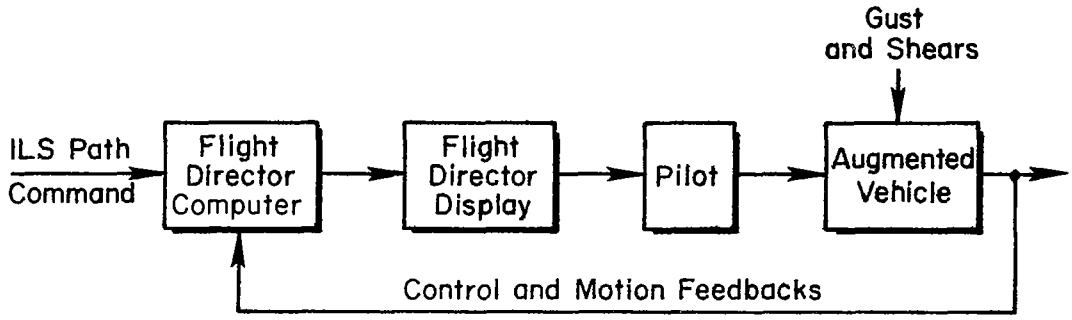

Figure 1. Flight Director System Elements for Landing Approach

The status information on the display indicates the aircraft state relative to the external world. This includes an artificial horizon for all purpose use, and other pictorial information pertinent to a particular phase of flight. For example, in the landing approach phase localizer and glide path signals are presented, and the more modern instruments also indicate altitude and airspeed error.

The nub of the dynamic design problem for flight director systems is the selection of the appropriate mix of signals to make up the steering commands. Historically, this mixture has been determined in two general ways:

- By adapting and displaying the output of an automatic flight control system
- By mechanizing the flight director computer based on guidance and control requirements, and adjusting the various feedback gains during simulation and flight test for acceptable pilot opinion and overall system performance.

Both approaches satisfy the overall system requirements for stability, path following, and regulation against disturbances. The first also offers the advantage of a nearly one to one correspondence with the automatic flight control system and can serve as a monitoring device for automatic operation. The second emphasizes the pilot as an active system element rather than as a monitor and backup. Neither of the approaches pay explicit attention to the specifics of the human pilot-centered characteristics until the system is tested or simulated with actual pilots.

This is undesirable, both economically and philosophically. Setting up a flight director system using ad hoc, ground-based and flight experimentation exclusively is much more costly than if the experimental program and data interpretation are guided by an adequate theory. Also, when flight director control is contrasted with other manual control modes, such as pilot operation on raw data from the full panel, the advantages of the flight director are primarily pilot-centered. Consequently, these advantages should be considered in terms of the relevant pilot properties from the very outset of design instead of as a final tuning up procedure which makes do with what is available. Among the advantages possessed by a flight director system which takes into account these pilot properties are:

- Reduction of pilot remnant (unwanted control action) by reducing scanning and the need for pilot equalization
- Reduction of pilot equalization
- Provision for a wide range of pilot gain to permit good characteristics with either loose or tight control.

All lead to superior control.

The theory of manual control displays permits the pilot-centered requirements to be considered at the design stage along with the usual guidance and control aspects. This theory derives from a large body of analytical and experimental research on

- Compensatory and pursuit control tasks
- Multiloop pilot response properties
- Pilot scanning and control behavior

It is still evolving and no single source summarizes all of its current aspects. An overview is provided by Refs. 1-5. The first reference summarizes the overall theory and methods of analysis. Reference 2 is primarily an example contracted from Ref. 1. References 3 and 4 present recent experimental research involving pilot control with instrument scanning. The latter includes some scanning data for flight director tasks. Reference 5 is the latest detailed account of the theory, and

it includes an illustrative example of pilot plus flight director control synthesis for a turbine helicopter.

The theory of manual control displays consists of the techniques, data, and models needed to analyze and design vehicle control systems whose elements are

- Man, as the controller
- Manipulator and feel systems
- Basic vehicle dynamics
- Stability augmentation systems
- Control and motion feedbacks; their sensing and shaping
- Pilot displays.

The theory is now developed sufficiently to be applied to several classes of problems, including the design of flight director systems. Specifically, given the effective controlled element consisting of the augmented vehicle, application of the theory permits the user to estimate:

- Vehicle motion quantities necessary as display inputs to the pilot
- Equalization and weighting of these display signals
- Predicted pilot dynamics — describing function plus remnant
- Expected pilot commentary and rating
- Measures of excess pilot workload capacity (e.g., as performance on a secondary task)
- System performance.

Other results of the theory which are important for the full panel but which are not central to an integrated flight director display include predictions of

- Instrumentation fixation probabilities and links
- Instrument dwell times
- Sensory workload.

C. SCOPE OF THIS REPORT

This report starts with the results and implications of the manual control theory of displays as a fundamental background. It proceeds directly to a definition of flight director system requirements, and from these requirements forms the basis for the analytical design procedure in this particular application of the display theory. The emphasis is on the feedback control system aspects of the flight director/vehicle system as a whole. In terms of system hardware, this impacts primarily on the flight director computer because this is where the intermix of signals occurs. The selection and design of the flight director display instrument format and its optimization from a human factors standpoint (e.g., symbol shape, illumination, etc.) are separate topics. Other assumptions which define the scope herein include the following:

- Longitudinal axis of control is emphasized
- Path command is an ILS glide slope
- Properties of the vehicle and its augmenters are known
- Needed feedbacks* can be sensed and/or synthesized using complementary filtering or other techniques.

Although longitudinal control is emphasized, the requirements in Section II have general applicability. The analytical techniques of Section III also apply by direct analogy to lateral path following. To make the analogy work one must translate into the terms of the lateral-directional equations of motion, and recognize some minor inner-loop differences; but the important point is that the resultant vehicle-plus-flight director controlled element as seen by the pilot must have dynamic properties similar to the longitudinal.

The primary concern of this report is with the selection of feedbacks and their weighting and equalization in the flight director computer. It involves the application of four general considerations or criteria, i.e.,

---

*Acquisition of all the feedbacks considered in the report is within the current state of the art.

- The system should possess adequate guidance and control properties (regulation, beam following, etc.)
- The dynamic response of the effective vehicle-plus-director controlled element (as seen by the pilot) should minimize the equalization and gain adjustment demands imposed on the pilot.
- The command signal should induce acceptable vehicle response when the pilot closes the loop.
- The displayed signals should be internally consistent and correspond with the real world, i.e., they should have a high degree of face validity.

These requirements are developed and elaborated in Section II.

Section III develops analytical design techniques for an advanced longitudinal flight director as a function of the vehicle properties and the requirements for longitudinal control in landing approach. It also considers the mechanizational aspects (e.g., antenna location) that influence the idealized case, as well as the use of additional control means (e.g., direct lift control, autothrottles) to increase the flight director potential.

The summary and conclusions comprise Section IV. Appendix A lists the vehicle equations and numerical values for the illustrative design example in Appendix C. Appendix B contains a derivation of the steady-state guidance and control properties. Appendix D presents examples of current director instrument face designs.

SECTION II

FUNCTIONAL REQUIREMENTS

The primary mission in landing approach is to arrive at the Category II window with the state variables of the aircraft and controller within acceptable limits. This is generally accomplished by acquiring the ILS beam early in the approach and following it to the window, all the while maintaining the aircraft near the average beam center in spite of external disturbances and beam noise. Landing is normally accomplished manually using visual cues. Landing can also be performed automatically, or manually on instruments, by continuing down the beam (or a smoothed extrapolation) to the flare initiation point and thence, following the flare computer's output, to touchdown.

The design requirements for the guidance and control system necessary to accomplish the approach are dictated by the following needs:

- Stability
- Following of the beam command
- Regulation against disturbances
- Compatibility with the human pilot

The satisfaction of these needs is the consideration which leads to the selection, sensing, shaping, and relative weighting of appropriate feedbacks in a way which is best for manual control using the flight director. The requirements can be grouped into those which are:

- Fundamental, and independent of whether the controller is an automatic or human pilot; and
- Human centered, and relate to the fact that the controller is a man.

These are elaborated below for longitudinal control.

A. FUNDAMENTAL REQUIREMENTS

The first set of requirements are independent of the type of controller, manual or automatic. In general, they are to establish the aircraft on

glide path, and to reduce any path errors to zero in a stable, well-damped and rapid manner. They lead to outer loop feedbacks which are those required to accomplish the mission. Additional inner loop feedbacks are needed to permit the first set of feedbacks to function. The basic system for longitudinal control is shown in Fig. 2.

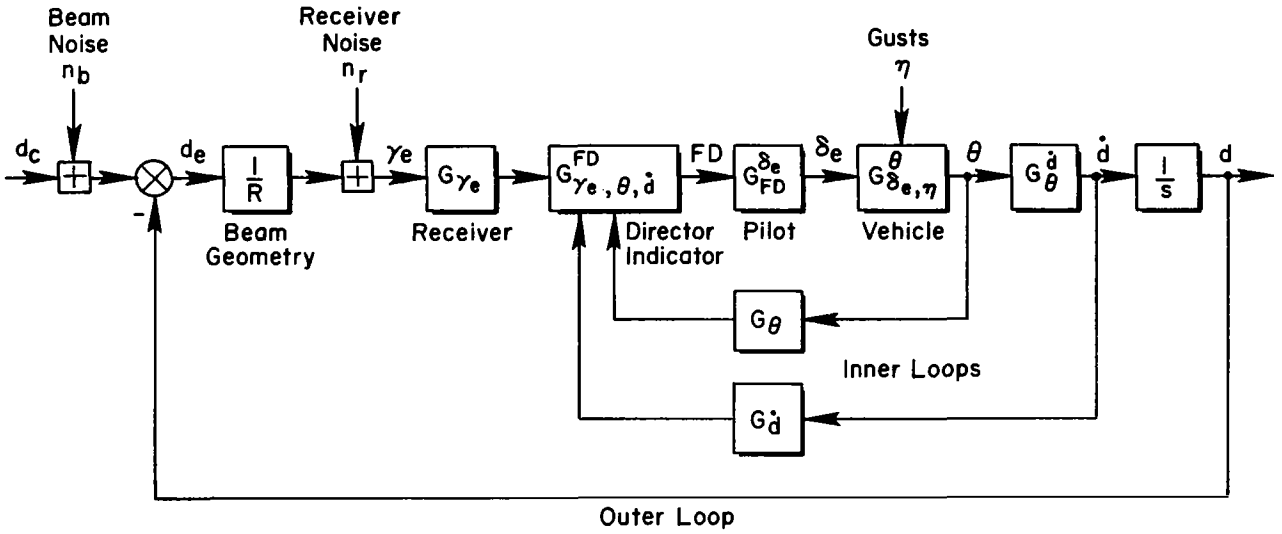

Figure 2. Block Diagram for Approach Control with Flight Director

The fundamental path quantity in the block diagram is the beam deviation, d_e, which is equal to the difference between the aircraft's altitude (at the antenna) and the instantaneous centerline of the beam. This is corrupted from the ideal by beam bends and noise in the airborne equipment. The actual physical signal is a glide path error angle, γ_e, converted from the deviation by the (decreasing) range to the receiver, R. The path error and the inner loop feedbacks are combined in the flight director computer and displayed to the pilot on the director indicator. The pilot can conceivably close other loops using raw data from the instrument panel, but these are unnecessary if the director is properly designed.

The equations of motion for the system in Fig. 2 are time varying due to the range variation, which is linear for constant speed. This

time variation requires compensation to provide an approximately constant effective controlled element, so that precision path control can be maintained throughout a director approach. This is done by inserting a range-varying gain as one of the operations in G_{γ_e} such that $G_{\gamma_e}/R = G_{d_e}$, where G_{d_e} is a constant-coefficient operator.

Inputs which lead to path errors may be deterministic or random. Deterministic input examples include:

- Step (offset) glide slope command, including initial beam acquisition.
- Dual angle beam, representing a ramp change from one beam angle to another.
- Configuration and trim changes in the vehicle (flap actuation, lowering gear, etc.).
- Discrete changes in the horizontal and vertical winds, including increasing or decreasing headwinds and tailwinds, i.e., shears.

Random inputs can include horizontal and vertical gusts, and beam bends and receiver noise. Their entry points to the system are shown in Fig. 2.

Table I summarizes the fundamental guidance and control requirements of the pilot/director/vehicle system. The right column lists the feedbacks to the flight director which can satisfy these requirements for the system functions which must be performed. Many of these are justified in Appendix B. Beam deviation provides the basic outer loop for command following, and its gain determines the bandwidth or stiffness of the system. Damping is achieved by feeding back functions of the attitude and/or beam rate. Pitch angle also has a primary function in maintaining attitude-stability and avoiding overrotations. Windproofing (path regulation against wind inputs) is accomplished by adding various functions of beam deviation. Integral of beam deviation avoids path errors in the presence of low frequency beam commands or wind shears, but its use in the flight director computer is not compatible with some pilot-centered requirements (Section B).

TABLE I

SUMMARY OF FEEDBACKS TO SATISFY FUNDAMENTAL REQUIREMENTS

SYSTEM FUNCTIONS — FUNDAMENTAL REQUIREMENTS	FLIGHT DIRECTOR FEEDBACKS
Path command and stiffening	Beam deviation, d
Path angle trimming	Beam integration, $\int d\ dt$
Curved path following	Beam double integration, $\int(\int d\ dt)dt$
Path damping	Attitude, θ, at path frequencies; or beam rate, $\dot{d}$; or rate of climb, $\dot{h}$
Short-period attitude regulation	Attitude, θ, at short-period frequencies
Short-period damping	Attitude rate, $\dot{\theta}$
Low frequency windproofing	Beam integration, $\int d\ dt$
Mid-frequency windproofing	Beam rate, $\dot{d}$; or rate of climb, $\dot{h}$
High frequency windproofing	Vertical acceleration, a_z

A preliminary illustration that these feedbacks satisfy the requirements can be given for the path mode, which becomes a second-order system when an equalizing inner loop is closed with a large gain. Assuming a high-gain pitch attitude inner loop, the block diagram of Fig. 2 reduces to that of Fig. 3 in the frequency region of pilot control. If the range variation is removed (or ignored, as when fixed-gain conditions are assumed) the equations for Fig. 3 are constant coefficient, and they can be Laplace transformed to give:

$$\left[\frac{G_\theta T_{\theta_2}}{U_o}\, s^2 + \left(G_{\dot{d}} + \frac{G_\theta}{U_o}\right)s + G_{d_e}\right]d \;=\; G_{d_e}\left[d_c + n_b + Rn_r\right] \qquad (1)$$

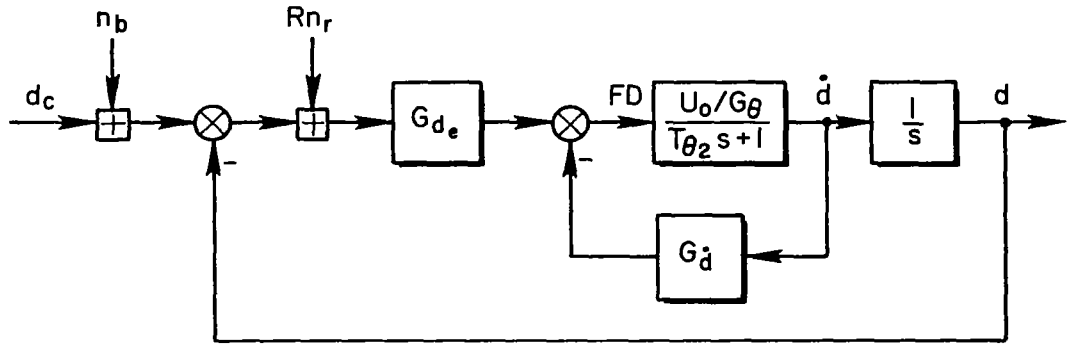

Figure 3. Path Mode Approximation
for Longitudinal Approach Control

When the transfer functions G_θ, $G_{\dot{d}}$, and G_d are pure gains, K_θ, $K_{\dot{d}}$, and K_d, the undamped natural frequency of the path mode is given by:

$$\omega_n = \sqrt{\frac{K_d U_o}{K_\theta T_{\theta_2}}} \tag{2}$$

The total damping becomes

$$2\zeta\omega_n = \frac{K_\theta + U_o K_{\dot{d}}}{K_\theta T_{\theta_2}} \tag{3}$$

The desired stiffness and damping are achieved by adjusting the feedback gains. A more complete development is given in Section III.

B. PILOT RELATED REQUIREMENTS

The presence of a human pilot in the control loop places additional requirements on the specification and design of the flight director. Two aspects are important. The first is the division of functions between the pilot and the flight director computer. At least some of the system functions are better satisfied by the pilot than by computer action. Second, the presence of the pilot in the loop adds another dimension to system performance considerations. The feedbacks must be selected, equalized

and weighted, not only to obtain good overall system performance, but also to be compatible with good subjective pilot ratings.

The pilot-centered requirements can be grouped for convenience as follows:

- Equalization to minimize pilot effort
- Response compatibility
- Face validity and command bar consistency.

These are elaborated below.

1. Equalization for Minimum Pilot Effort

The desire to minimize pilot effort while retaining maximum system performance imposes requirements on the dynamic properties of the effective controlled element consisting of the vehicle plus flight director computer. As is very well known, the human pilot adapts his characteristics to compensate for the dynamic deficiencies of the effective controlled element. As part of this adaptation, he may be forced to develop low-frequency lead(s) and/or to adjust his gain precisely. When low-frequency lead is required of the pilot, a cost in pilot dynamic capacity is incurred (Refs. 6-8); which is reflected in increased effective time delay and remnant. Increases in both these quantities cause a deterioration in system performance and pilot ratings. To some extent, the increased time delay can be reduced by increasing the neuromuscular system tension. This, too, has a substantial cost in increased pilot effort. Finally, while it is possible for the pilot to maintain his gain and other dynamic properties relatively constant when such precision adjustment is required, the additional cockpit workload which can be handled is reduced.

As a result of these human pilot properties, an obvious design requirement is that the effective control element be constructed to:

- Require no low frequency lead equalization
- Permit pilot loop closure over a wide range of gains.

This can be achieved when the effective controlled element approximates either a pure gain, K, or a pure integration, K/s, over the frequency range of pilot/director/vehicle system crossover. For the pure gain case, the pilot must adopt a very low frequency lag equalization; this corresponds to a slow trim-like operation and is not objectionable. However, the dynamics of an aircraft between elevator and attitude are not a gain, and it is not feasible to attain this without additional automatic feedbacks to augment the vehicle dynamics. With the basic vehicle plus flight director, a pure gain controlled element at low frequencies might be obtained, for example, by shaping the ILS signal with a large lead (i.e., differentiator). This would result in an undesirable amplification of glide slope noise. Another possibility is to include a very high gain elevator feedback to the flight director. In this case, the large feedback gain requires a reduction in display scale, thereby making the desired command inputs barely perceptible to the pilot. Higher gain elevator feedback also violates the "face validity" requirement discussed below.

An effective controlled element consisting of an integrator, K/s, is nearly as good as a pure gain from the standpoint of pilot response and performance in single-loop tasks. It has distinct advantages over the latter as a basis for the design of flight director computers. For this set of controlled element dynamics the pilot response is approximately a gain plus time delay in the frequency region of control (near crossover). His time delay will be close to minimum, and the remnant can be minimized with the proper choice of controlled element gain. Pilot lead generation requirements are small, although the pilot can use a small amount of high-frequency lead to reduce his effective time delay in the loop. This lead can be minimized by making the controlled element less than a K/s at high frequencies, e.g., with a small amount of elevator feedback.

In short, the key requirement is to adjust the weightings of the various motion feedbacks in the flight director computer so that the effective controlled element approximates the K/s form over a fairly

broad frequency region. At the same time, achieving a K/s effective controlled element is the way to satisfy most of the fundamental requirements presented in Section A.

Other requirements based on minimizing pilot effort include the following:

- Filter the pilot's output (particularly if high frequency feedbacks are used) to avoid undesirable disturbance due to remnant. Ordinary manual control system dynamics are usually sufficient to accomplish this action.

- Range compensate the beam error so that the display/controlled element dynamics are approximately time invariant. The pilot can adjust to nonstationary situations, but it involves adaptation and learning which increases task difficulty and degrades performance.

- Account for other pilot workload and for unattended operation by providing effective controlled element amplitude ratio and phase characteristics that permit wide variations in pilot gain while retaining adequate gain and phase margins throughout the mid-frequency region. This implies that conditionally stable systems, and feedback of beam integral are undesirable.

These requirements and their feedback implications must be further tempered with the considerations for response compatibility and command bar consistency.

2. Response Compatibility

The response compatibility requirements relate to the ways in which the various motions of the aircraft interrelate and how they affect the pilot. With a flight director present the important cues are combined into a net "error" signal which the pilot attempts to reduce to zero by manipulating the controls. When this is done the airframe motions generated by the pilot should be similar to those which he experiences under other manual control conditions. This is desirable both for the pilot's internal self-monitoring functions and for the monitoring of pilot activity by the copilot using the full instrument panel. To achieve response compatibility, the feedbacks used in the nondirector situation should be present in the flight director signal — beam deviation, pitch attitude, and altitude rate.

One way to describe response compatibility characteristics quantitatively is with the use of modal response ratios. Imagine, for instance, that the aircraft has been displaced from the beam and that the flight director system is operating to reduce this departure, then the Laplace transforms of the beam response will be given by

$$d(s) = \frac{d_o}{s} + \frac{d_1}{s - s_1} + \frac{d_2}{s - s_2} + \cdots + \frac{d_N}{s - s_N} \tag{4}$$

where the s_i's are the roots of the closed loop characteristic equation of the flight director system and the beam forcing function. Then the Laplace transform of other aircraft motion quantities such as attitude, θ, or normal acceleration, a_z, will be

$$\theta(s) = \frac{d_o}{s}\left[\frac{\theta(s)}{d(s)}\right]_{s=0} + \frac{d_1}{s - s_1}\left[\frac{\theta(s)}{d(s)}\right]_{s_1} + \frac{d_2}{s - s_2}\left[\frac{\theta(s)}{d(s)}\right]_{s_2} + \cdots + \frac{d_N}{s - s_N}\left[\frac{\theta(s)}{d(s)}\right]_{s_N}$$

$$a_z(s) = \frac{d_o}{s}\left[\frac{a_z(s)}{d(s)}\right]_{s=0} + \frac{d_1}{s - s_1}\left[\frac{a_z(s)}{d(s)}\right]_{s_1} + \cdots + \frac{d_N}{s - s_N}\left[\frac{a_z(s)}{d(s)}\right]_{s_N} \tag{5}$$

The bracketed quantities in Eq. 5 are modal response ratios. In general they have both an amplitude ratio and a phase. The closed loop response in a well designed flight director system will be dominated by only a very few (3 or less) basic modes. These will be associated with the system crossover region. The values of s_i within that region are measures of the system bandwidth.

To carry the example further, consider that the crossover frequency is at a location where the short period equations of motion are approximately valid and that the modal response ratio relating flight path and attitude is pertinent. Under these conditions θ/γ would be given by Eq. 6.

$$\frac{\theta}{\gamma} \doteq \left[T_{\theta_2} s + 1\right]_{s_i} \tag{6}$$

Thus if the dominant modes, s_i, are such that $|T_{\theta_2} s_i| << 1$, then attitude and path are related on a nearly proportional, in fact one to one, basis. On the other hand, if the system crossover frequency is considerably higher, such that $|T_{\theta_2} s_i| >> 1$, then the attitude will be much greater than the flight path change in this mode.

Now, let us translate all of this back to the response compatibility in recovering the beam centerline from an offset. With adequate damping presumed, this will be accomplished most rapidly if the system bandwidth is very large. While the response in "d" would then be very good, the associated attitude and load factor responses may be much greater than the pilot or passengers desire — an incompatible situation. This can be avoided by specifying allowable or desirable values of pertinent modal response ratios. In turn, for a given aircraft and control system technique, these specifications would limit the maximum system bandwidth. Unfortunately there are no hard data on the key modal response ratios for flight director or automatic landing systems. Presumably, the value of $|\theta/\gamma|_{s_i}$ for the dominant modes should be near unity to avoid overrotation in corrective maneuvers. As a practical matter, this is not as important on flight director systems as on automatic approach systems because the modal response ratios of the dominant mode, and hence response compatibility, are ultimately set by the gain the pilot uses in closing the loop. It is a central issue in pilot/vehicle system performance predictions.

Another related requirement is the compatibility of the flight director with the autopilot during an automatic approach. Ideally such compatibility might be taken to mean that the signals driving the autopilot servo and the signals to the flight director should only differ by a gain. Unfortunately, certain signals such as the integral of beam deviation are appropriate for the automatic system but not for the flight director. These minor differences need not be significant since the primary goal would be to make the autopilot and flight director correspond only at the dominant automatic flight control system modes. But this implicitly requires that the modal response ratios exhibited by the flight director system be compatible with those of the automatic system.

3. Face Validity and Command Bar Consistency

Some elements of a flight director display are intended to reproduce, instrumentally, portions of the external world which are sources of visual flight cues. To the extent that the resulting abstraction evokes responses while on IFR that are similar to responses under VFR conditions, the display is adequate from a behavioral standpoint. Of course the IFR abstraction may be superior to VFR in principle by providing cues which are difficult or impossible for the pilot to obtain from the visual scene. On flight directors, these cues are used as command signals which the pilot is to follow. The remainder of the display presents status information which, ideally, has a one-to-one correspondence with the actual situation. In this sense the status information has a high degree of "face validity" with the outside world. For example, the artificial horizon, except for any registration errors, corresponds directly with the actual horizon. Other status elements that tend to show a similar one-to-one correspondence are the glide slope and localizer signals. Figure 4 illustrates this aspect of "face validity" of the status elements. It shows a line drawing of the status elements of the typical flight director instrument (based on the summary in Appendix D). The status information is generally realistic and easy to interpret.

The command signals, which are our major concern in this report, must also have some aspects of face validity. But the cue here is different from status information in that the command signal is a mixture of control and vehicle motions so there is no corresponding real-world cue. However, some correspondence does exist between the command signal and the vehicle or control motions in each of several frequency bands. In each band, the flight director command may be dominated by a particular airplane motion or control quantity. So, even though there is no VFR cue which corresponds directly to the flight director command, nonetheless the command signal must have some degree of consistency with the status elements on the display and thus the pilot's visual world view. The types of consistency needed are best illustrated by a series of examples.

If the integral of beam deviation is made one component of the command signal in an attempt to reduce a steady-state beam error to zero, and the

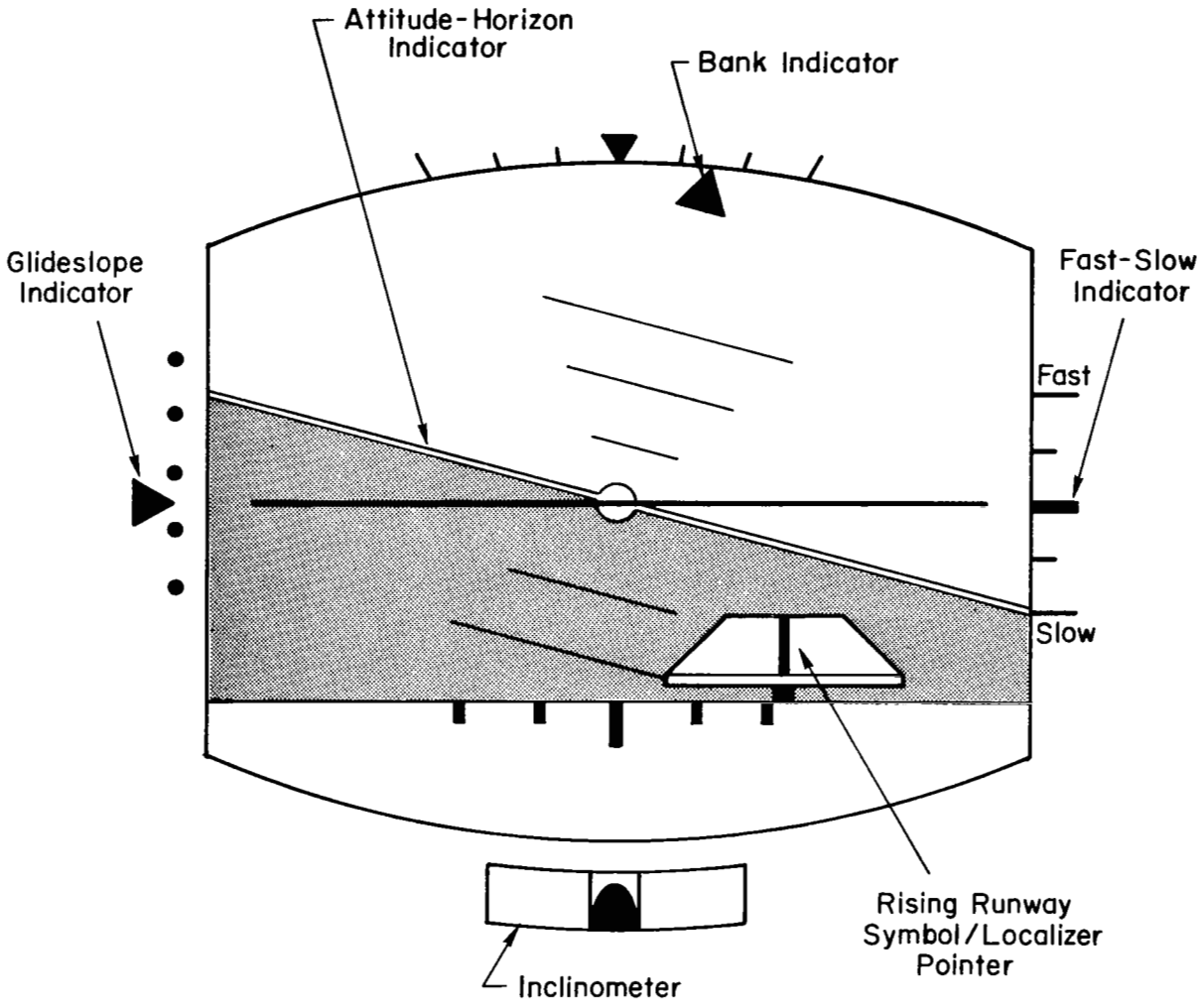

Figure 4. Presentation of Status Information on a Modern Flight Director Indicator

pilot operates intermittently on this signal, then a flight director command can develop during the periods of unattended operation if the aircraft is just slightly off the beam. When the pilot closes the flight director loop, this acts as an initial condition which must be countered by reducing the output of the beam integrator. If the aircraft were quickly maneuvered to reduce the beam deviation to zero, the displayed command signal would not be zero. Thus the integral of beam deviation is not a suitable component of the flight director command signal because it can result in a displayed low frequency error when the aircraft is actually stabilized on the beam. In this sense, the command would be inconsistent with the status information of the ILS indicator. This example is not only a question of face validity, but is also a situation where the guidance and control requirements would not be met because of the pilot's intermittent behavior. The integral component is also undesirable because it could drive the command indicators to saturation when the flight director is turned on, or during long periods of unattended operation.

Since the integral of beam deviation cannot be used for the several reasons noted above, the lowest frequency component of the command signal should be beam deviation itself. If pitch attitude feedback is used as a means to supply path damping, and if there is no washout of this signal, then the command bar can be zero if the beam deviation and pitch attitude components are equal and opposite. The indication would be that the aircraft was on the beam, whereas the fact would be quite different. In this case, it would be inconsistent for the glide slope and artificial horizon status information to indicate the aircraft was not on glide path while, at the same time, the command bar was zero. This is, again, a situation where face validity and command bar consistency are faulty. To alleviate this the pitch angle signal component should be zero at low frequencies, yet provide a signal proportional to θ in the short-period frequency region.

From considerations of equalization to minimize pilot effort, response compatibilities, and face validity and command bar consistency, a number of flight director computer requirements have been described. These are summarized in Table II.

TABLE II

FLIGHT DIRECTOR COMPUTER FUNCTIONS
FOR PILOT-CENTERED REQUIREMENTS

REQUIREMENT	FUNCTION
K/s effective controlled element	$\dot{h}$ feedback at mid-frequency
Lead and remnant minimization	δ_e feedback (with lag) at mid- to high frequencies
Command bar consistency	Only d feedback at very low frequency. θ feedback at short period frequencies.
Response compatibility	Response with flight director similar to that for raw data (or VFR); and similar to that for autopilot, i.e., θ and $\dot{h}$ inner loop feedbacks.

Taken together, the guidance and control and pilot-centered requirements prescribe the flight director computer feedbacks, as well as the general nature of their weighting and equalization, needed to accomplish a landing approach in the presence of disturbances. The implementation and analytical interpretation of these requirements for conventional transport-type aircraft are presented in Section III.

SECTION III

ANALYTICAL DEVELOPMENT OF ADVANCED LONGITUDINAL DIRECTOR

A central part of this report is the derivation of an effective controlled element consisting of the vehicle-plus-flight director computer which will satisfy both the guidance and control and the pilot-centered requirements outlined in Section II. This is accomplished in this section by setting up a rudimentary system, and subjecting it to constructive criticism. Then, taking the criticism into account, a more advanced system is evolved, and the critical routine is repeated. This sequential process also highlights the effects on the controlled element dynamics of selection, equalization, and weighting of the feedbacks.

The axes system and vehicle equations are specified at the outset. The analysis begins with a basic system which has feedbacks that satisfy the functional requirements in a minimal way: beam deviation plus washed-out pitch attitude. Although this basic system is adequate, significant improvements can be made by introducing additional feedbacks and equalization in the director computer. The result is a composite system that has superior path regulation and command following properties, and which satisfies the pilot's subjective feeling for responsiveness, validity, and consistency.

Elevator is considered to be the primary control. The effects of throttle and direct lift control on the effective vehicle dynamics are discussed where appropriate.

The following analyses are done in generic terms. They are illustrated in Appendix C by a numerical example for a DC-8 aircraft in landing approach.

A. AXIS SYSTEM AND VEHICLE EQUATIONS

The basic block diagram for the pilot/director/vehicle system is given in Fig. 2. The vehicle element is summarized below as a preface to the flight director computer development.

A conventional body-fixed stability axis system is used. In landing approach the unperturbed x-axis is aligned with the glide slope, making $\theta_o = \gamma_o$ as shown in Fig. 5. Due to the body-fixed nature of the axis

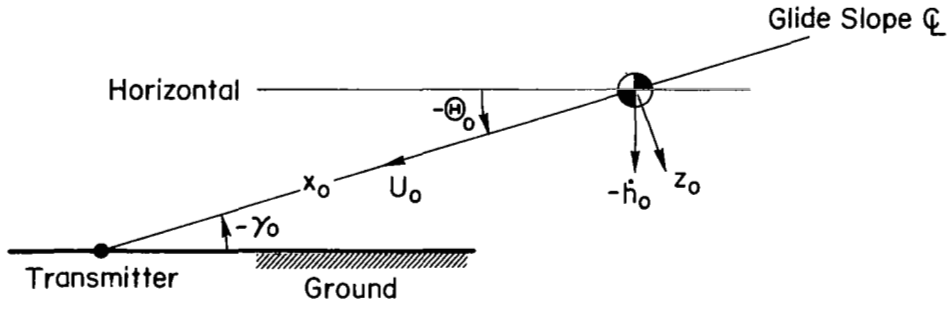

Figure 5. Initial Axis System Alignment

system, perturbations in aircraft attitude change the orientation of the x- and z-axes as shown in Fig. 6.

Beam deviation, d, is normal to the glide slope, while altitude, h, is measured vertically, positive up. When the initial x-axis is not horizontal, it is important to differentiate between d and h. For example, in a headwind there is a reduction in groundspeed when the pilot holds airspeed constant.

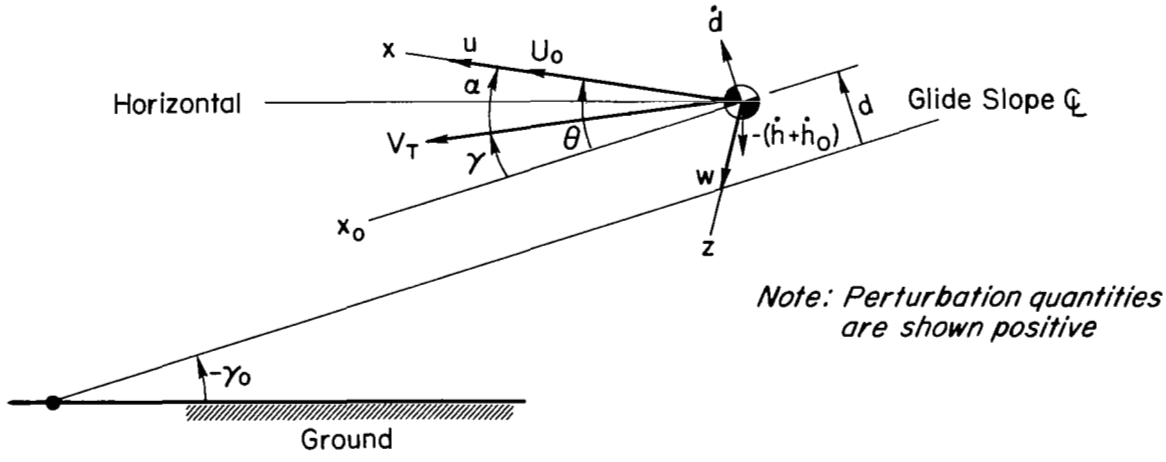

Figure 6. Perturbed Axis System Alignment

There must therefore be a corresponding reduction (perturbation) in the rate of descent, $\dot{h}$, in order to maintain a constant inertially referenced glide path angle. The result is a zero beam rate deviation, but a constant altitude rate perturbation. Beam deviation, d, and altitude, h, will be distinguished in the analysis where appropriate.

The longitudinal dynamics of the vehicle are assumed to be described by the linearized 3-degree-of-freedom perturbation equations given in Eq. 7.

$$\begin{bmatrix} s - X_u & -X_w & g\cos\Theta_o \\ -Z_u & s - Z_w & -U_o s + g\sin\Theta_o \\ -M_u & -(M_{\dot{w}} s + M_w) & s(s - M_q) \end{bmatrix} \begin{bmatrix} u \\ w \\ \theta \end{bmatrix} = \begin{bmatrix} X_{\delta_e} & X_{\delta_T} & -X_\eta \\ Z_{\delta_e} & Z_{\delta_T} & -Z_\eta \\ M_{\delta_e} & M_{\delta_T} & -M_\eta \end{bmatrix} \begin{bmatrix} \delta_e \\ \delta_T \\ \eta \end{bmatrix} \tag{7}$$

$$\dot{d} = -w + U_o\theta + \ell_x\dot{\theta} \text{ , at station } \ell_x$$

$$\dot{h} = -w\cos\Theta_o + u\sin\Theta_o + U_o\cos\Theta_o\theta$$

$$a_z = \dot{w} - U_o\dot{\theta} + g\sin\Theta_o\theta - \ell_x\ddot{\theta} \text{ , at station } \ell_x$$

The terms are defined in the list of symbols. Appendix A contains a detailed description of the characteristic equation, transfer functions, short-period approximations, and steady-state gust responses derived from this set of equations.

B. THE BASIC BEAM-DEVIATION-PLUS-PITCH-ATTITUDE SYSTEM

A minimum system which meets the guidance and control requirements of Section II for conventional aircraft consists of beam deviation and pitch attitude feedbacks to the director computer. This deviation/attitude system is shown in the block diagram of Fig. 7, where G_h^{FD} and G_θ^{FD} are the respective feedback functions.

The system is assumed to be linearized by removing the range variation; i.e., letting $G_{\gamma_e} \doteq KR$ in Fig. 2 so that $G_{h_c}^{FD}$ is a constant in Fig. 7. Also,

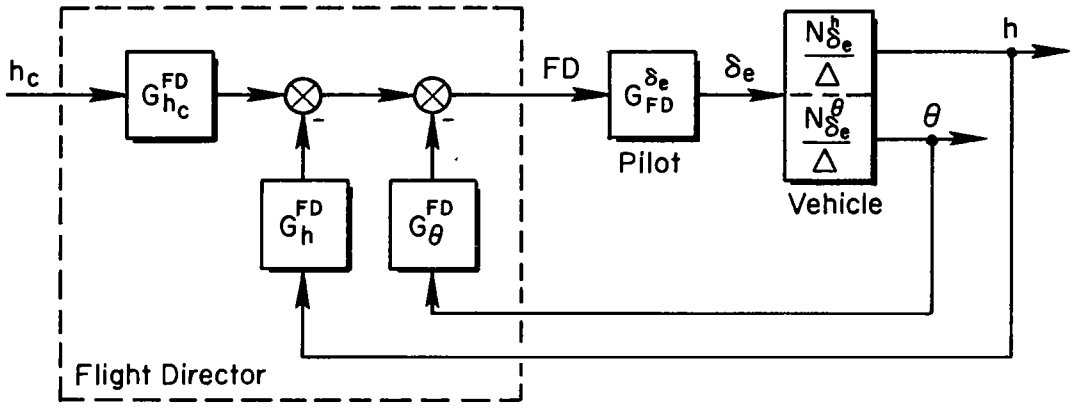

Figure 7. Simplified Flight Director System Block Diagram

deviation, d, has been simplified to perturbation altitude, h, by assuming no steady-state wind effects to change the groundspeed . Without wind, the small difference between d and h due to sin Θ_o and cos Θ_o is negligible for glide path angles of current ILS systems.

Distinction is made between $G^{FD}_{h_c}$ and G^{FD}_h in Fig. 7 to permit separation of the equalization of the ILS data from that of the vehicle's internal measuring system. Both blocks contain ILS data but feedbacks that are not referenced to the beam (e.g., rate of climb and normal acceleration) are added in the feedback block only.

1. Steady State Regulation and Command Following

The deficiencies of the basic deviation/attitude system provide one basis for evolving the form and function of an advanced director. Among the deficiencies are those related to very low frequency (approaching steady state) requirements for path following and gust regulation (wind-proofing). Inputs with which the pilot/director/vehicle system may be expected to cope include the following:

- Step offset from the beam
- Change in beam angle
- Curved beam
- Step changes in wind velocity
- Ramp changes in wind velocity (shears).

Steady-state analyses in Appendix B examine the response of the basic system to these types of inputs, and draw implications for additional equalization or feedbacks. The result of these analyses is the list of alternative minimum systems for each type of input given in Table III. The 2-degree-of-freedom case assumes that the pilot controls elevator while airspeed is held constant with autothrottle (or pilot control). The 3-degree-of-freedom case involves only elevator control with airspeed allowed to vary.

The wind shears and curved beams are seen to result in the most complex systems. Comparing the 2- and 3-degree-of-freedom cases indicates that autothrottle simplifies the minimum director, generally removing the need for pilot elevator trim.

The need in some cases for beam integration within the director computer is in conflict with pilot-centered requirements for display consistency. This can be handled in several ways, including

- Full time beam integration with limiting.
- Multi-mode flight director, in which beam integration is switched in when needed.
- Providing other status information to permit the pilot to perform more than a single integration.

Similarly, the need for rapid attitude washout to give good low and mid-frequency windproofing tends to conflict with the path damping requirement, and this compromise is treated subsequently.

2. Director plus Vehicle as an Effective Controlled Element

The requirements of Section II and the steady-state considerations noted above define a number of feedbacks to the flight director computer. A central implication of the pilot-centered requirements is that the gains and equalizations be selected so that the net dynamics from pilot elevator output to director instrument displacement look approximately like an integration, K/s. The analytical procedure for assessing and establishing this result is given below for the basic deviation/attitude system. The deficiencies of this basic system then lead to a more advanced system evolved in the rest of Section III.

TABLE III

MINIMUM SYSTEMS FOR STEADY-STATE BEAM ERROR WITH DISCRETE INPUTS

INPUT	MINIMUM SYSTEMS	
	CONSTANT AIRSPEED (2 D.F.)	VARIABLE AIRSPEED (3 D.F.)
Step beam	Beam deviation only; Eq. B-8	Beam deviation only; Eq. B-7
Dual angle beam	Beam deviation; plus washed-out θ or beam integration; Eq. B-8	Beam deviation; plus washed-out θ and pilot elevator trim, or beam integration; Eq. B-7
Curved beam	Beam deviation; plus washed-out θ and beam integration; Eq. B-8	Beam deviation; plus washed-out θ and pilot elevator trim and beam integration; Eq. B-7
Step w-gust	Beam deviation; plus washed-out θ or beam integration; Eq. B-14	Beam deviation; plus beam integration, or washed-out θ and pilot elevator trim, Eq. B-13
Shear w-gust	Beam deviation; plus washed-out θ and beam integration; Eq. B-14	Beam deviation; plus washed-out θ and pilot elevator trim and beam integration; Eq. B-13
Step u-gust	Beam deviation only.	Beam deviation only; Eq. B-19
Shear u-gust	Beam deviation; plus pilot throttle trim	Beam deviation; plus washed-out θ and pilot elevator trim, or beam integration; Eq. B-19

The dynamics of the effective controlled element as seen by the pilot can be obtained by adding the component vehicle motion transfer functions with their associated equalization. The effective flight director transfer function is then

$$\frac{FD}{\delta_e} = \frac{G_\theta^{FD} N_{\delta_e}^{\theta} + G_h^{FD} N_{\delta_e}^{h}}{\Delta} \tag{8}$$

For the basic system, the feedback functions are initially constant, so

$$G_\theta^{FD} = K_\theta \tag{9}$$

$$G_h^{FD} = K_h \tag{10}$$

The controlled element transfer function is given by:

$$\frac{FD}{\delta_e} = \frac{K_\theta A_\theta \left(s + \frac{1}{T_{\theta_1}}\right)\left(s + \frac{1}{T_{\theta_2}}\right) + K_h \frac{A_h^{\cdot}}{s} \left(s + \frac{1}{T_{h_1}}\right)\left(s + \frac{1}{T_{h_2}}\right)\left(s + \frac{1}{T_{h_3}}\right)}{\Delta} \tag{11}$$

The vehicle numerators are given in Appendix A. A simplified expression valid in the region of pilot control is obtained by eliminating the high frequency terms.* This results in

$$\frac{FD}{\delta_e} \equiv \frac{K_\theta A_\theta \; s \left(s + \frac{1}{T_{\theta_1}}\right)\left(s + \frac{1}{T_{\theta_2}}\right) + K_h A_h^{\cdot *} \left(s + \frac{1}{T_{h_1}}\right)}{s\Delta} \tag{12}$$

where $A_h^{\cdot *} = A_h^{\cdot}\left(\frac{1}{T_{h_2}}\right)\left(\frac{1}{T_{h_3}}\right) = -Z_\alpha M_{\delta_e}$

The numerator of Eq. 12 combines into a first-order root at nearly $1/T_{h_1}$ and a second-order pair at an undamped natural frequency, ω_θ, proportional

*This assumes the effect of Z_{δ_e} is negligible at frequencies less than ω_{sp}.

to the $\sqrt{K_h/K_\theta}$ gain ratio. The approximate transfer function is:

$$\frac{FD}{\delta_e} \doteq \frac{K_\theta A_\theta \left(s + \frac{1}{T_{h_1}'}\right)\left[s^2 + 2\zeta_\theta \omega_\theta s + \omega_\theta^2\right]}{s\left[s^2 + 2\zeta_{sp}\omega_{sp} s + \omega_{sp}^2\right]\left[s^2 + 2\zeta_{sp}\omega_{sp} s + \omega_{sp}^2\right]} \tag{13}$$

where $$\omega_\theta = \sqrt{\frac{K_h A_{\dot{h}}^*}{K_\theta A_\theta}} = \sqrt{\frac{-K_h Z_\alpha}{K_\theta}} \tag{14}$$

$$\zeta_\theta = \frac{1}{2T_{\theta_2}} \sqrt{\frac{K_\theta A_\theta}{K_h A_{\dot{h}}^*}} \tag{15}$$

Figure 8 contains frequency response ($j\omega$-Bode) and root locus plots of this basic system transfer function for two values of the gain ratio, K_h/K_θ. The smaller value is given by the dashed line. The location of the ω_θ zeros is determined by the ratio $\sqrt{K_h/K_\theta}$. Note that at larger K_h/K_θ values (solid line) the system is conditionally stable and has no region of K/s-like amplitude ratio. This will make the system more sensitive to variations in pilot gain, and will restrict the pilot-vehicle system crossover to frequencies outside the crosshatched unstable region. The system becomes stable over a broad region as ω_θ is decreased. Also, as ω_θ is decreased the spread between ω_θ and ω_{sp} increases, and a region of K/s-like amplitude ratio is produced in between. As such, there is less sensitivity to changes in pilot gain; i.e., with K/s-like dynamics the form of the response is invariant with change in gain and the bandwidth is proportional to the gain selected, while with K/s^2-like systems the closed-loop dynamics change sharply as the gain varies. The systems of Fig. 8 will have a high frequency instability point beyond ω_{sp} due to higher-order lags in the display, actuator, and pilot.

a. Pitch Attitude Washout

The basic system of Fig. 8 contains "pure" pitch attitude feedback. Windproofing considerations showed that attitude feedback must be washed out at low frequency, i.e.,

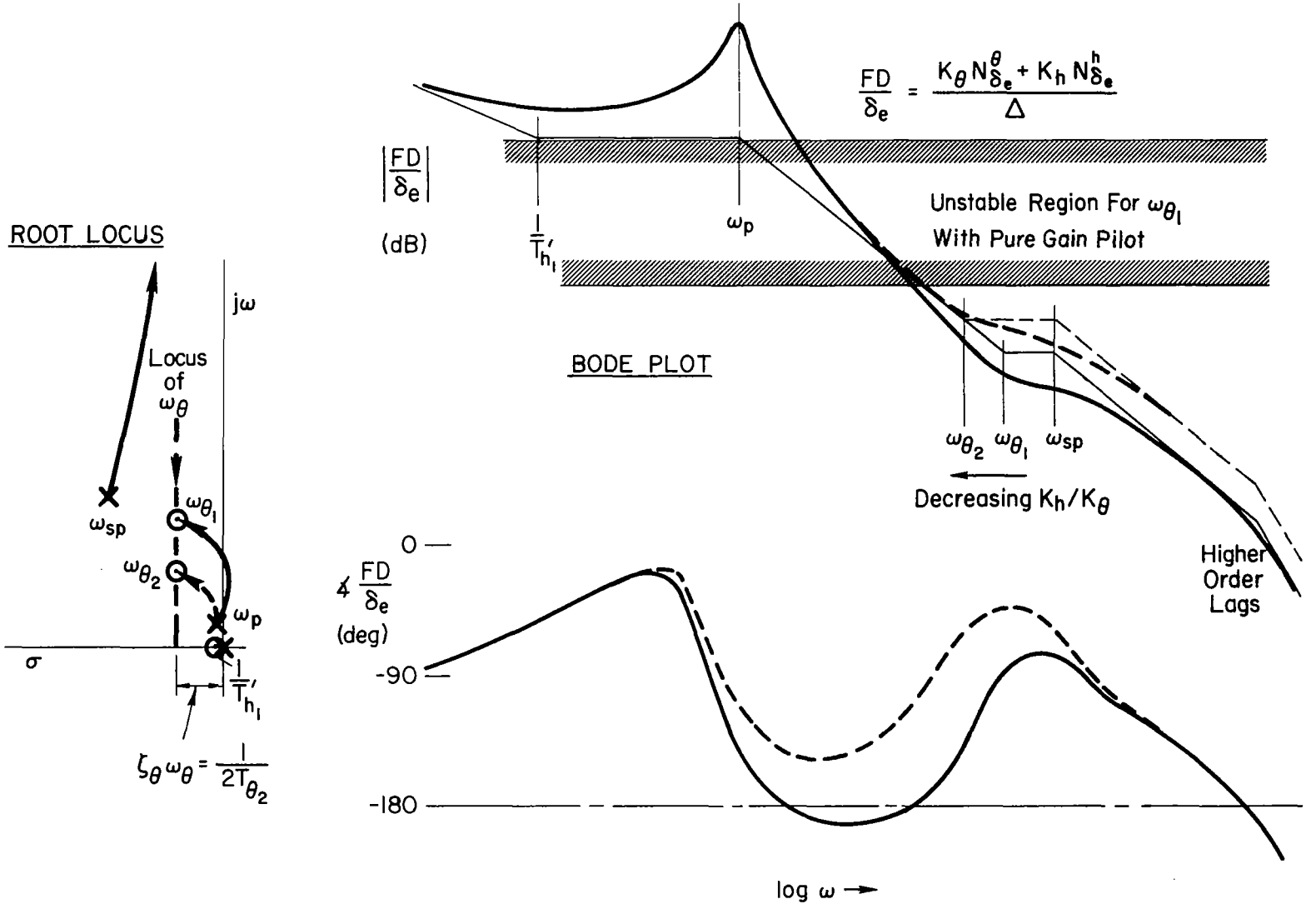

Figure 8. Variation in Director Vehicle Properties with K_h/K_θ Weighting

$$G_{\theta}^{FD} = \frac{K_{\theta}s}{\left(s + \frac{1}{T_{WO}}\right)} \tag{16}$$

For adequate path damping, however, a good attitude signal must be retained at and below mid-frequencies. In order to obtain a closed-loop system that will have the required windproofing as well as having the closed-loop path mode at a frequency greater than the phugoid, the washout inverse time constant must be less than the phugoid, ω_p. With approach speeds on the order of 200 to 300 fps, the washout time constant will generally be around 10 sec. Such a low frequency washout does not materially change the approximate flight director transfer function of Fig. 8. Faster time constants will reduce the damping of the ω_θ zeros below that shown in Fig. 8. For example, if the washout time constant was equal to T_{θ_2}, the ω_θ zeros would be on the imaginary axis and the highest crossover frequency would be near the vehicle phugoid.

b. Speed Control with Throttle

In the three-degree-of-freedom case, flight director control with only elevator does not provide stable operation below the speed for minimum drag; i.e., during "backside" operation. Even above this speed there can be an appreciable delay before the airplane motions naturally return to their trim condition. This lag is related to the low frequency closed-loop mode at approximately $1/T_{h_1}$ (in the altitude-to-elevator numerator, $N_{\delta_e}^{\dot{h}}$), which moves into the right half plane for backside operation. To reduce the time delay, $1/T_{h_1}$ must be moved further into the left half plane. Elevator control will not modify $1/T_{h_1}$, and the conventional way to augment it is by control with the throttle.

The desired effect of the throttle loop is to improve the altitude numerator, given by

$$\frac{1}{s} N_{\delta_e}^{\dot{h}}\Big]_{u \rightarrow \delta_T} = \frac{1}{s}\left(N_{\delta_e}^{\dot{h}} + K_u N_{\delta_e \delta_T}^{\dot{h}\, u}\right)$$

The second term on the right is the throttle loop gain times the coupling numerator. The effect on $1/T_{h_1}$ of increasing K_u is shown in the root locus sketch. The main effect on the characteristic

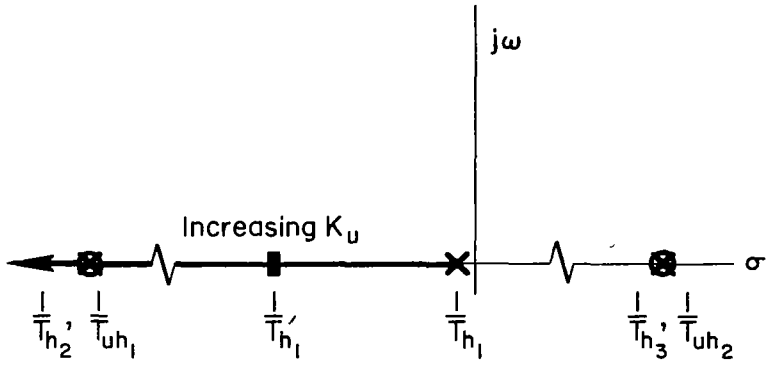

Altitude Numerator Root Locus

equation (denominator) is to damp the phugoid, yielding the two degree of freedom model in the limit. These effects will effectively make the controlled element form in Fig. 8 a K/s^2 at very low frequency. Hence, autothrottle is required if the aircraft is below the speed for minimum drag and it serves to increase the path damping.

c. Deficiencies of the Basic Deviation/Attitude System

The most apparent drawback of a basic h, θ flight director system is the K/s^2 nature of the effective controlled element in the anticipated crossover frequency region between the phugoid, ω_p, and short period, ω_{sp}. This does not adequately meet the pilot-centered requirement derived in Section II for a K/s-like amplitude response.

Referring to Fig. 8 and Eqs. 14 and 15, it can be seen that with large enough pitch gain, K_θ, the second order ω_θ zeros can be overdamped to produce two first order zeros. Although this might appear to improve the mid-frequency gain and produce the desirable K/s region, it has several drawbacks. First, since the total damping, $\zeta_\theta\omega_\theta$, is constant the two first orders may not be

placed separately in the most desirable locations. Secondly, the flight director will look very much like an amplified pitch attitude display, and be quite "busy" in turbulence. This violates command bar consistency, and attempts by the pilot to follow the bar will result in unacceptable normal accelerations and pitch attitude excursions — incompatible response.

Other overall deficiencies of the basic θ, h flight director include poor gust regulation due to the slow attitude washout, and high sensitivity of the ω_θ zeros to slight changes in the K_h/K_θ ratio. Keeping K_h/K_θ precisely constant requires a linear desensitization of the glide slope signal as range decreases. This is a difficult mechanizational task to do exactly, and as a result, a conditionally stable system may be produced during some portions of the approach.

The amplitude ratio in Fig. 8 has a K/s^2-slope above the short period. This implies a need for pilot (or other) lead equalization in this frequency range, in order to extend the K/s region. Usually, this will not be a strong requirement, unless ω_{sp} is smaller than about 1 rad/sec. For lower short period frequencies, additional equalization in the director should be considered.

The advantages and deficiencies of the attitude/beam deviation system are summarized in Table IV. Attention now turns toward overcoming these deficiencies with a more advanced system.

C. ADDITION OF BEAM RATE FEEDBACK TO THE BASIC DIRECTOR

Combining beam rate with attitude and beam deviation feedbacks provides the basis for an advanced director which has several advantages. These include more precise beam following, improved gust regulation, and better fulfillment of pilot-centered requirements.

1. Steady-State Regulation and Command Following

The steady-state beam deviation equations are the same as those derived in Appendix B for the basic system unless altitude rate, $\dot{h}$, is used in place of true beam rate, $\dot{d}$. With $\dot{h}$ the functional blocks,

TABLE IV

RELATIVE PROPERTIES OF THE BASIC
DEVIATION/ATTITUDE FLIGHT DIRECTOR

ADVANTAGES	DEFICIENCIES
Simple to mechanize Provides command bar consistency with washed out attitude feedback	K/s^2-like amplitude ratio at mid-frequency when K_h/K_θ weighting is acceptable Poor w-gust windproofing due to slow washout K/s^2-like amplitude ratio at high frequency Maximum crossover frequency restricted by non-pilot lags in forward loop

G_h^{FD} and $G_{h_c}^{FD}$, of Fig. 7 are no longer equal, and a $G_{\dot{h}}^{FD}$ feedback must be added to G_h^{FD}. The result can be seen in the following three-degree-of-freedom steady-state expressions for beam error due to beam command, w-gust, and u-gust.

$$d_e\Big]_{ss} = \lim_{s\to 0} s\left[\frac{s(G_{TD}^{\delta_e FD}G_\theta^\theta C_{\delta_e} + E_\Delta + G_{FD}^{\delta_e FD}G_{\dot{h}}^{d} D_{\delta_e})}{G_{FD}^{\delta_e FD}G_d^d D_{\delta_e}}\right] d_c(s) \qquad (17)$$

$$d_e\Big]_{ss} = \lim_{s\to 0} s\left[\frac{D_{w_g}^{d} + G_{FD}^{\delta_e}(G_\theta^{FD}B_{\delta_e w_g}^{\theta\, d} + G_{\dot{h}}^{FD}C_{\delta_e w_g}^{u\, \dot{d}})}{G_{FD}^{\delta_e FD}G_d^d D_{\delta_e}}\right] w_g(s) \qquad (18)$$

$$d_e\Big]_{ss} = \lim_{s\to 0} s\left[\frac{G_{\dot{h}}^{FD}C_{\delta_e u_g}^{u\, \dot{d}}}{G_d^{FD}D_{\delta_e}^{d}}\right] u_g(s) \qquad (19)$$

The numerator coefficients are given in Appendix A. Note that $G_{\dot{h}}^{FD}$ operates on $\dot{h}$ feedback. All free s terms have been multiplied through.

The requirements for $G_{\dot{h}}^{FD}$ are the same as for G_{θ}^{FD}, including washout. However, the beam error to u-gust transfer function no longer has a numerator free s. This will then cause a standoff to u_g and w_g shears, unless beam integral is included in the G_d^{FD} control path. However, the constant term in the d_e for u_g input expression, Eq. 19, is generally quite small, so the resulting steady-state error to a u_g shear may be negligible.

2. Director Plus Vehicle as an Effective Controlled Element

The general equation for the h, θ, $\dot{h}$ director is

$$\frac{FD}{\delta_e} = \frac{G_h^{FD} N_{\delta_e}^{h} + G_{\theta}^{FD} N_{\delta_e}^{\theta} + G_{\dot{h}}^{FD} N_{\delta_e}^{\dot{h}}}{\Delta} \tag{20}$$

The dynamic features of this combined system show a broad K/s-like region between the phugoid and short period. It allows faster attitude washout than does the basic system. These results are developed below.

Combining $\dot{h}$ and θ changes the second-order zeros* in the flight director transfer function of Eq. 13 to

$$\left[s^2 + \left(\frac{1}{T_{\theta_2}} + \frac{K_{\dot{h}}}{K_{\theta}} \frac{A_{\dot{h}}^{*}}{A_{\theta}} \right) s + \frac{K_{\dot{h}}}{K_{\theta}} \frac{A_{\dot{h}}^{*}}{A_{\theta}} \right] \tag{21}$$

Again, $1/T_{h_2}$ and $1/T_{h_3}$ are assumed large relative to ω_{sp}. This quadratic may be separated into two independent first order zeros, each located independently to maximize the K/s region. This means placing them at ω_p and ω_{sp}, respectively.

Placement of the zeros is facilitated by an approximation for the roots of Eq. 21 when the two roots are greatly different. They are one small root

*The $\dot{h}$ washout is assumed to have an inverse time constant at or below phugoid frequencies and it will not influence these mid-frequency zeros.

$$\frac{1}{T_1} = \frac{\frac{K_h Z_\alpha}{K_\theta}}{\left(\frac{1}{T_{\theta_2}} + \frac{K_{\dot{h}} Z_\alpha}{K_\theta}\right)} \doteq \frac{\frac{K_h Z_\alpha}{K_\theta}}{\frac{K_{\dot{h}} Z_\alpha}{K_\theta}\left[1 - \frac{K_\theta}{U_o K_{\dot{h}}}\right]} \doteq \frac{K_h}{K_{\dot{h}}} \tag{22}$$

and one large root,

$$\frac{1}{T_2} = -\frac{K_{\dot{h}} Z_\alpha}{K_\theta}\left[1 - \frac{K_\theta}{U_o K_{\dot{h}}}\right] \doteq -\frac{K_{\dot{h}} Z_\alpha}{K_\theta} \tag{23}$$

Figure 9 presents frequency response and root locus plots for the modified director/vehicle controlled element. The zeros have been located as follows:

$$\frac{1}{T_1} \doteq \frac{K_h}{K_{\dot{h}}} \doteq \omega_p \tag{24}$$

$$\frac{1}{T_2} \doteq -\frac{K_{\dot{h}} Z_\alpha}{K_\theta} \doteq \omega_{sp} \tag{25}$$

The frequency response shows a broad K/s region between ω_p and ω_{sp}, with very little phase dip near ω_p. The path damping is now coming from the low frequency zero, $1/T_1$, due to the $\dot{h}$ feedback. Good high frequency properties are provided by the other zero, $1/T_2$.

a. Pitch Attitude Washout

With the addition of $\dot{h}$, the attitude feedback can be washed out much faster than in the basic flight director case without compromising the mid-frequency path damping. This will improve the low frequency windproofing. The relationship between θ and $\dot{h}$ is helpful in determining the slowest reasonable pitch attitude

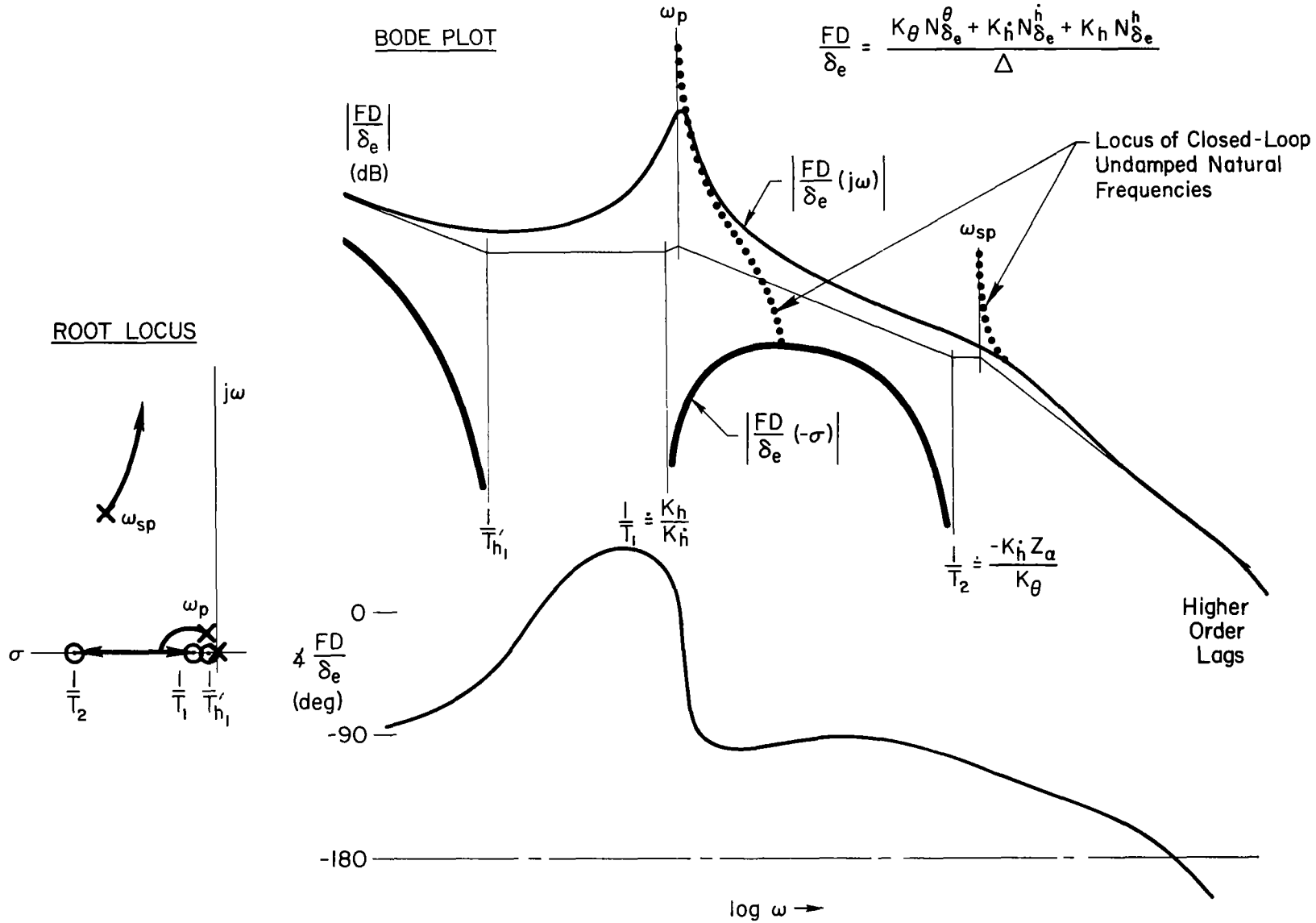

Figure 9. Director/Vehicle Properties with Beam Rate Added

washout time constant. In the low to mid-frequency region, a good approximation relating $\dot{h}$ and θ for elevator inputs is given by

$$\frac{\dot{h}}{\theta} = \frac{U_o}{T_{\theta_2}s + 1} \tag{26}$$

Thus, for frequencies below $1/T_{\theta_2}$, $\dot{h}$ and θ feedbacks are redundant (in the absence of winds), and θ can be washed out with a time constant of at least T_{θ_2}. Because the pitch attitude feedback provides the required attitude stability, the ultimate lower limit on the washout time constant is near the short period frequency.

The effect of the washout location on the low frequency windproofing can be shown analytically as follows. Rewrite the effective controlled element transfer function, FD/δ_e, to include an attitude washout, T_{WO}. The numerator of this transfer function becomes:

$$N_{\delta_e}^{FD} = \frac{K_\theta A_\theta s\left(s+\frac{1}{T_{\theta_1}}\right)\left(s+\frac{1}{T_{\theta_2}}\right)}{\left(s+\frac{1}{T_{WO}}\right)} + \frac{K_{\dot{h}}A_{\dot{h}}\left(s+\frac{1}{T_{h_1}}\right)\left(s+\frac{K_h}{K_{\dot{h}}}\right)\left(s+\frac{1}{T_{h_2}}\right)\left(s+\frac{1}{T_{h_3}}\right)}{s} \tag{27}$$

Assuming, as before, that the high frequency altitude zeros are large with respect to the short period frequency, Eq. 27 simplifies to

$$N_{\delta_e}^{FD} \doteq \frac{K_\theta A_\theta s^2\left(s+\frac{1}{T_{\theta_1}}\right)\left(s+\frac{1}{T_{\theta_2}}\right) + K_{\dot{h}}A_{\dot{h}}^*\left(s+\frac{1}{T_{WO}}\right)\left(s+\frac{1}{T_{h_1}}\right)\left(s+\frac{K_h}{K_{\dot{h}}}\right)}{s\left(s+\frac{1}{T_{WO}}\right)} \tag{28}$$

The summation of numerator terms in Eq. 28 is illustrated by the root locus sketches in Fig. 10. The "closed-loop" numerator washout, $1/T_{WO}$, moves around with the "open-loop" value, $1/T_{WO}$. The flight director transfer function approximation becomes

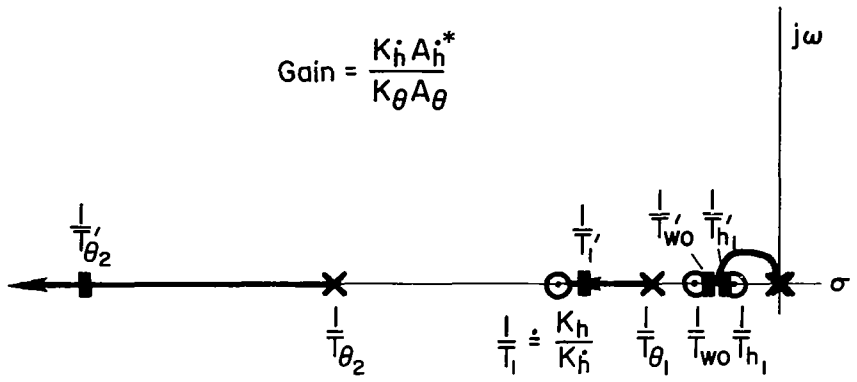

a) Slow Washout

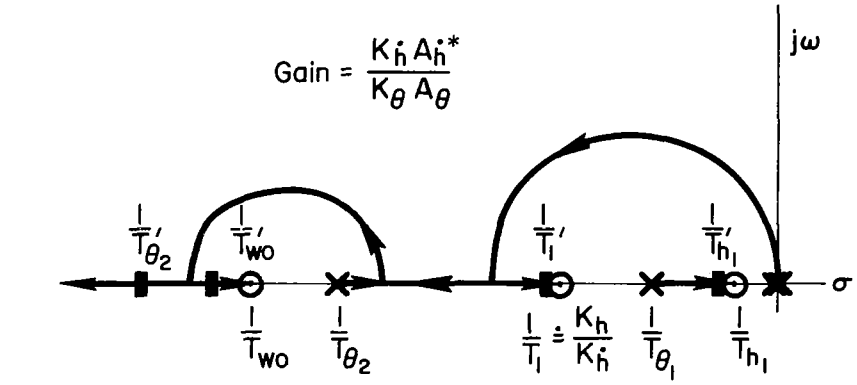

b) Fast Washout

Figure 10. Locus of Zeros of Director/Vehicle Numerator

$$\frac{FD}{\delta_e} \doteq \frac{K_\theta A_\theta \left(s + \frac{1}{T'_{h_1}}\right)\left(s + \frac{1}{T'_{WO}}\right)\left(s + \frac{1}{T'_1}\right)\left(s + \frac{1}{T'_{\theta_2}}\right)}{s\left(s + \frac{1}{T_{WO}}\right)\Delta} \qquad (29)$$

The numerator and denominator washout terms form a dipole pair which occurs at low or high frequency in Fig. 10, depending on the washout time constant.

The washout dipole has little effect on the open-loop director/vehicle effective controlled element properties in Fig. 9, and the pilot loop closure properties will be essentially the same. Assuming

the same pilot crossover frequency (near the short period in Fig. 9) for the slow and fast washout cases, the beam command, d/d_c, responses will be about the same, but the low frequency gust responses will differ.

The washout modifies the closed-loop phugoid a little, moving it to a somewhat higher frequency in the fast washout case. The closed-loop w-gust numerator is obtained by adding the coupling numerator times the θ-loop equalization to the open-loop gust numerator, i.e.,

$$N^d_{w_g}\Big]' = N^d_{w_g} + \frac{K_\theta s}{\left(s + \frac{1}{T_{WO}}\right)} N^{d\,\theta}_{w_g \delta_e} \qquad (30)$$

It changes substantially with washout variation as shown in the Fig. 11 root loci (for increasing K_θ). A significant point in Fig. 11 is that the low frequency zeros in the fast case, ω'_{g_F}, can have a fairly low damping ratio, depending on ω_g and the effective θ-loop gain.

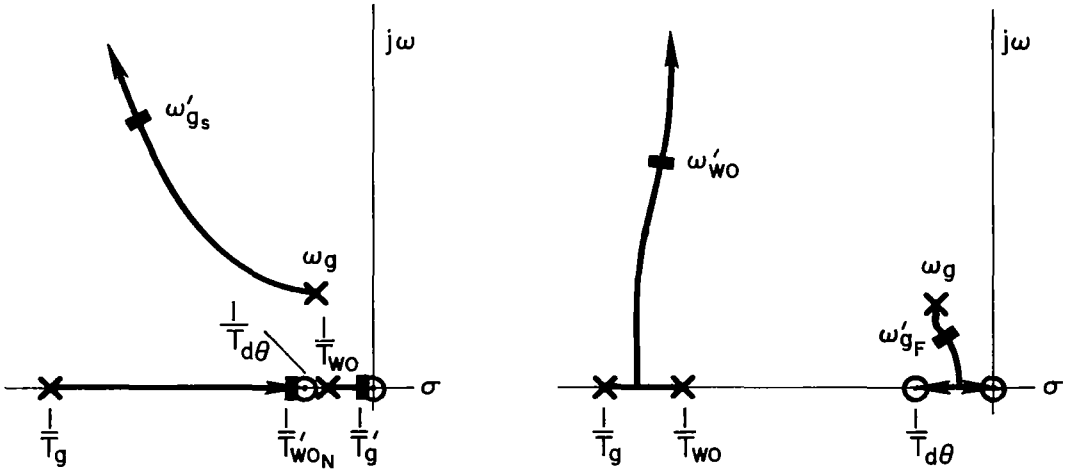

a) Slow Washout Locus

b) Fast Washout Locus

Figure 11. Effect of Pitch Attitude Washout on w-Gust Numerator Roots

The closed-loop beam error to w-gust transfer function can be obtained by combining the closed-loop characteristic roots (for a selected crossover on Fig. 9) with the closed-loop numerator from Eq. 30. The result in the slow washout case has the form

$$\left.\frac{d_e}{w_g}\right]_{FD\rightarrow\delta_e} = \frac{A_{wg}\left(s+\frac{1}{T'_g}\right)\left(s+\frac{1}{T'_{WO_N}}\right)\left[s^2+2\zeta'_{g_s}\omega'_{g_s}s+\omega'^2_{g_s}\right]}{\left(s+\frac{1}{T'_{h_1}}\right)\left(s+\frac{1}{T'_{WO_\Delta}}\right)\left(s+\frac{1}{T'_{p_1}}\right)\left(s+\frac{1}{T'_{p_2}}\right)\left[s^2+2\zeta'_{sp}\omega'_{sp}s+\omega'^2_{sp}\right]} \tag{31}$$

The closed-loop gust numerator in Eq. 31 includes a term at $1/T'_{WO_N}$ due to the washout, and three terms from the basic d/w_g numerator. The closed-loop denominator has a term due to the washout, $1/T'_{WO_\Delta}$, and the phugoid has been overdamped to give two real roots, $1/T'_{p_1}$ and $1/T'_{p_2}$. This response is plotted as the upper curve in Fig. 12.

$$\left.\frac{d_e}{w_g}\right|_{FD\rightarrow\delta_e} = \frac{N^d_{w_g}+G^{\delta_e}_{\theta}N^{d}_{w_g}{}^{\theta}_{\delta_e}}{\Delta+G^{\delta_e}_{\theta}N^{\theta}_{\delta_e}+G^{\delta_e}_{d}N^{d}_{\delta_e}}$$

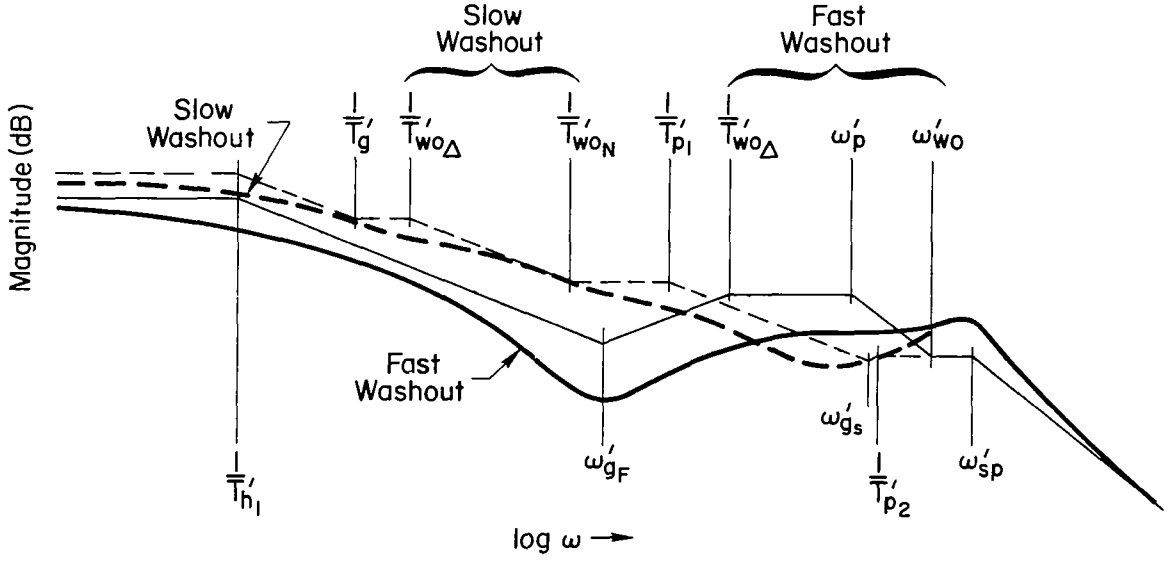

Figure 12. Effect of Pitch Attitude Washout on Beam Error Due to w-Gust

The generic closed-loop w-gust response transfer function for a relatively fast washout typically becomes:

$$\left.\frac{d_e}{w_g}\right]_{FD-\delta_e} = \frac{A_{w_g}\left[s^2 + 2\zeta'_{g_F}\omega'_{g_F}s + \omega'^2_{g_F}\right]\left[s^2 + 2\zeta'_{WO}\omega'_{WO}s + \omega'^2_{WO}\right]}{\left(s + \frac{1}{T'_{h_1}}\right)\left(s + \frac{1}{T'_{WO_\Delta}}\right)\left[s^2 + 2\zeta'_{p}\omega'_{p}s + \omega'^2_{p}\right]\left[s^2 + 2\zeta'_{sp}\omega'_{sp}s + \omega'^2_{sp}\right]} \tag{32}$$

The fast washout gust response is the lower curve in Fig. 12. Now the high frequency quadratic in the closed-loop numerator is affected by the washout, as shown in Fig. 11. The effective closed-loop phugoid is also different from that in Eq. 31, having been moved to higher frequency. The denominator washout term moves to higher frequency as expected.

The curves in Fig. 12 illustrate the well known result that faster pitch attitude washout reduces beam error due to low and mid-frequency gusts. The difference in error is related to the area between the curves on Fig. 12 when plotted in linear rather than logarithmic coordinates. As an example, if the w-gust is described by a low frequency first order power spectrum the difference in the mean square errors for the systems of Fig. 12 will be about a factor of two because the average separation of the amplitude ratios is about 3 dB. Note the important influence of the damping ratio, ζ'_{g_F}, of the low frequency numerator quadratic in the fast case.

b. The Use of Blended Direct Lift Control

For flight director control using elevator and throttle, the upper limit for the path mode bandwidth is given approximately by the high frequency pitch attitude numerator term, $1/T_{\theta_2}$. Blended direct lift control (DLC) which augments Z_{δ_e} in the basic vehicle can be used to increase $1/T_{\theta_2}$, potentially improving the path mode response. The pertinent block diagram is given in Fig. 13, where the DLC control is related to elevator action via a crossfeed, resulting in augmented vehicle dynamics.

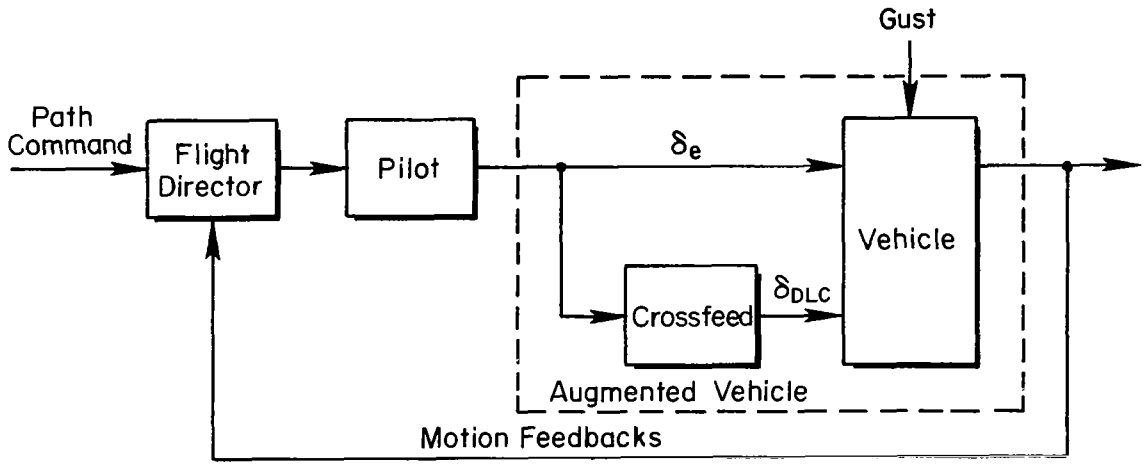

Figure 13. Block Diagram for Direct Lift Control

The primary effect of blended DLC occurs in the pitch attitude numerator, with secondary changes occurring in the high frequency part of the altitude numerator. The pitch attitude numerator with DLC becomes

$$N^{\theta}_{\delta_e}\Big]_{\delta_e \rightarrow \delta_{DLC}} = N^{\theta}_{\delta_e} + K_{DLC} N^{\theta}_{\delta_{DLC}} \qquad (33)$$

$N^{\theta}_{\delta_{DLC}}$ has the same form as $N^{\theta}_{\delta_e}$, i.e., two real zeros $1/T_{\theta_1}$ and $1/T_{\theta_2}$. In either numerator the low frequency zero is predominated by X_u, so $1/T_{DLC_1}$ is almost equal to $1/T_{\theta_1}$. The approximate factor for the other zero is

$$\frac{1}{T_{DLC_2}} = -Z_w + \frac{M_w}{M_{\delta_{DLC}}} Z_{\delta_{DLC}}$$

which moves from $1/T_{\theta_2}$ toward the right half plane as $Z_{\delta_{DLC}}$ is increased. The effect of increasing K_{DLC} is shown in the sketch of the locus of numerator roots. Increasing $1/T_{\theta_2}$ will increase $1/T_2$ in Fig. 9, which can be interpreted as augmenting Z_α in the

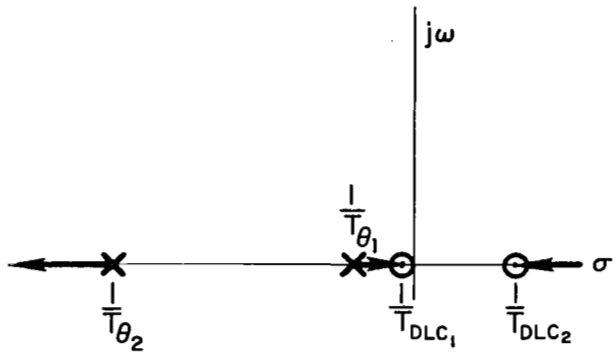

Pitch Numerator Root Locus

expression for $1/T_2$, i.e.,

$$\frac{1}{T_2} \doteq \frac{-K_{\dot{h}}(Z_\alpha + Z_{\delta_{DLC}})}{K_\theta}$$

The main result is to increase the bandwidth of the closed-loop beam command transfer function, d/d_c. In summary, while blended DLC is not a requirement for an advanced flight director, the resulting augmented vehicle dynamics should be used as the basis for the director analysis when DLC is included.

c. Deficiencies of the Beam-Rate-Added Director

The main remaining deficiency of the combined θ, h, $\dot{h}$ flight director system is that the desired K/s-like region of the effective controlled element does not extend beyond the short-period frequency. This means that potential high gain pilot closures will require pilot lead equalization in the vicinity of the short period. Means for offsetting this are discussed subsequently.

D. ADDITION OF PITCH RATE FEEDBACK TO THE ADVANCED DIRECTOR

The inclusion of pitch rate in G_θ^{FD} creates an additional zero in the flight director transfer function, FD/δ_e. Placing the zero near the short period makes the flight director transfer function K/s-like at and above

ω_{sp}. The closed loop short period damping ratio will then increase as the pilot increases his gain.

The effective flight director numerator can be formed by adding its component equalizations and numerators in the usual way.

$$N_{\delta_e}^{FD} = \frac{K_{\dot{\theta}} A_\theta s\left(s + \frac{1}{T_{WO}} + \frac{K_\theta}{K_{\dot{\theta}}}\right)\left(s + \frac{1}{T_{\theta_1}}\right)\left(s + \frac{1}{T_{\theta_2}}\right)}{\left(s + \frac{1}{T_{WO}}\right)} + \frac{K_{\dot{h}} A_{\dot{h}}^{*}\left(s + \frac{K_h}{K_{\dot{h}}}\right)\left(s + \frac{1}{T_{h_1}}\right)}{s} \tag{34}$$

Again, the high frequency terms in $N_{\delta_e}^{h}$ are neglected. If $\omega_{sp} >> \omega_p$, the approximate expression for the numerator becomes

$$N_{\delta_e}^{FD} = \frac{K_{\dot{\theta}} A_\theta\left(s + \frac{1}{T_{h_1}'}\right)\left(s + \frac{1}{T_1}\right)\left(s + \frac{1}{T_{WO}'}\right)\left[s^2 + 2\zeta_\theta \omega_\theta s + \omega_\theta^2\right]}{s\left(s + \frac{1}{T_{WO}}\right)} \tag{35}$$

where $\frac{1}{T_1} \doteq \frac{K_h}{K_{\dot{h}}}$, $2\zeta_\theta\omega_\theta \doteq \frac{1}{T_{\theta_2}} - \frac{Z_\alpha K_{\dot{h}}}{K_{\dot{\theta}}}$, and $\omega_\theta^2 \doteq -\frac{Z_\alpha K_{\dot{h}}}{K_{\dot{\theta}}}\left(\frac{1}{T_{WO}} + \frac{K_\theta}{K_{\dot{\theta}}}\right)$.

What was a first order lead (in Fig. 9) near the short period now becomes a second order at ω_θ.

A generic Bode-root locus plot for the revised director, Eq. 35, is given in Fig. 14. There is a broad K/s region from the phugoid to the higher order lags (display dynamics, etc.). The resulting closed-loop altitude response to beam commands for a possible pilot crossover frequency is shown by the dashed line on the jω-Bode plot. Both the closed-loop phugoid, ω_p', and the short period, ω_{sp}', are well damped, and there is little phase dip in FD/δ_e, so that the system is insensitive to gain changes.

There will be a closed-loop root at low frequency as the free s at the origin is driven to $1/T_{h_1}'$ (see $|FD/\delta_e(-\sigma)|$ on Fig. 14). Although

$$\frac{FD}{\delta_e} = \frac{(K_{\dot\theta} M_\delta - K_{\dot h} Z_\delta)(s + 1/T_{h_1}')(s + 1/T_1)\left[s^2 + 2\zeta_\theta \omega_\theta s + \omega_\theta^2\right]}{s\left[s^2 + 2\zeta_p \omega_p s + \omega_p^2\right]\left[s^2 + 2\zeta_{sp} \omega_{sp} s + \omega_{sp}^2\right]}$$

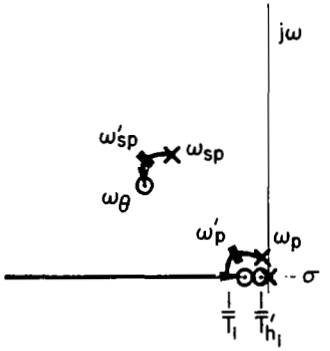

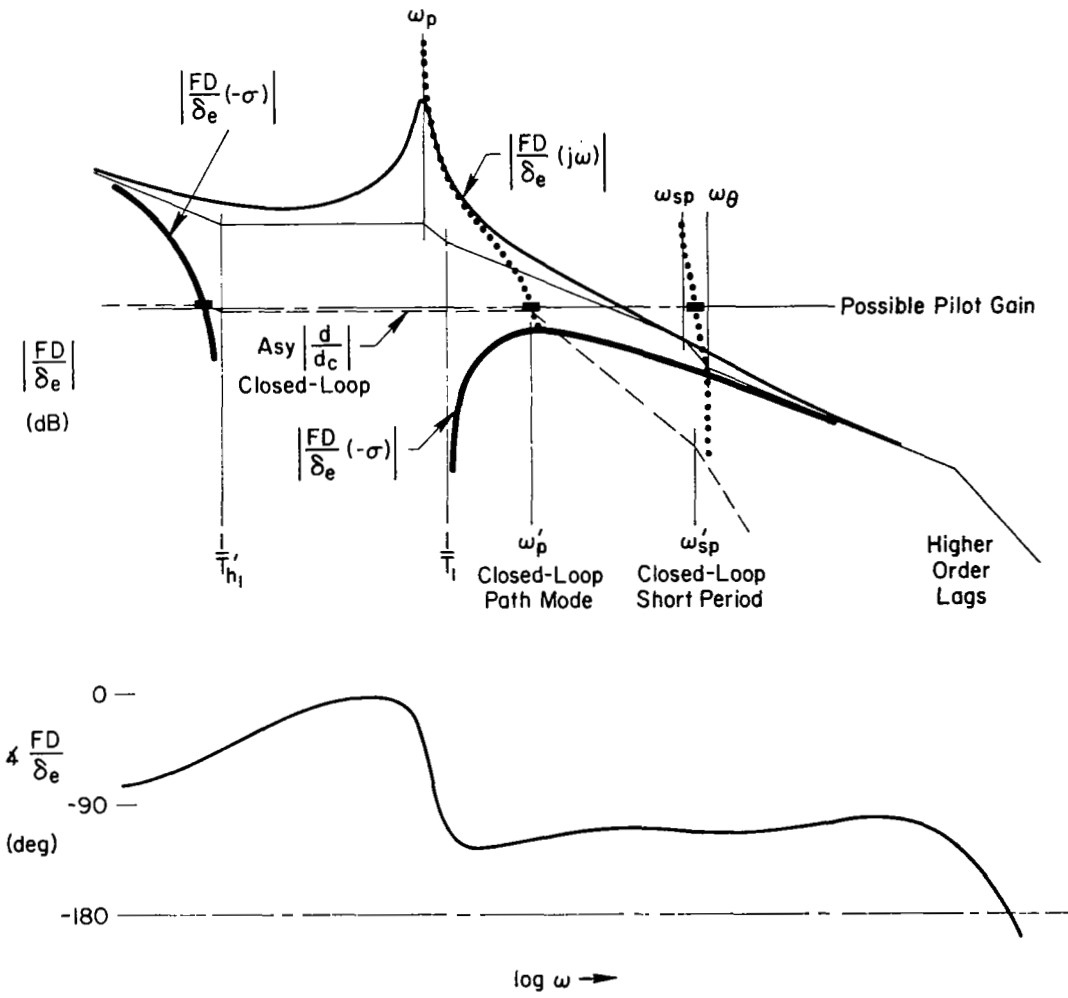

Figure 14. Director/Vehicle Properties with Pitch Rate Added

this root is nearly cancelled by the $1/T_{h_1}'$ zero in the closed-loop beam response there will be a significant modal response in the other vehicle motions, primarily airspeed. In other words, when the vehicle is disturbed from its trim condition the beam error will quickly return to zero but the airspeed will have a very long settling time. As brought out in Section B-2-b this settling time cannot be changed without separate throttle control.

E. ADDITION OF ELEVATOR FEEDBACK TO THE ADVANCED DIRECTOR

Another possible feedback to the director computer is elevator deflection. This introduces an additional functional box, $G_{\delta_e}^{FD}$, to the feedbacks in the Fig. 7 block diagram. The director/vehicle effective controlled element transfer function becomes

$$\frac{FD}{\delta_e} = \frac{\left[G_h^{FD} N_{\delta_e}^{h} + G_\theta^{FD} N_{\delta_e}^{\theta} + G_{\dot{h}}^{FD} N_{\delta_e}^{\dot{h}} + G_{\dot{\theta}}^{FD} N_{\delta_e}^{\dot{\theta}}\right] + K_{\delta_e}\Delta}{\Delta} \qquad (36)$$

when $G_{\delta_e}^{FD} = K_{\delta_e}$. The locus of numerator roots for increasing K_{δ_e} is given in Fig. 15. The result is a high frequency lead at $1/T_{\delta_e}$. The remaining numerator terms are relatively unchanged.

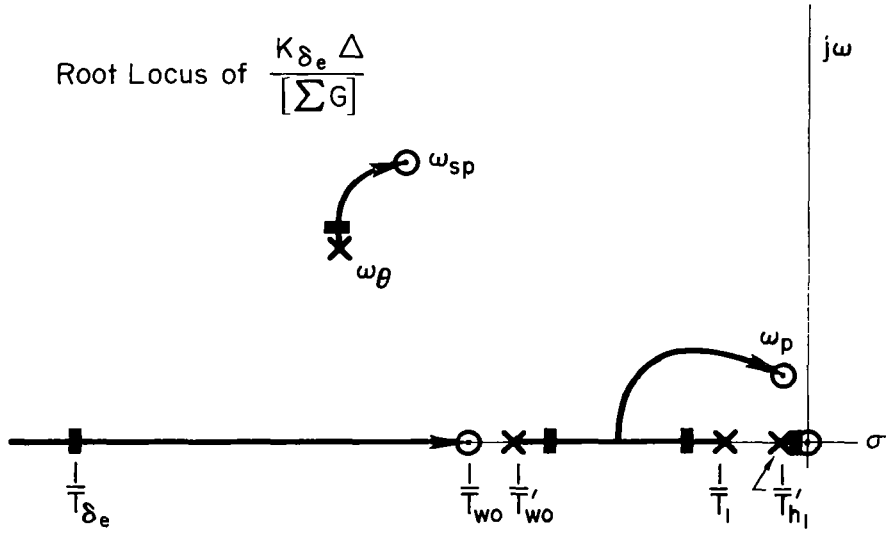

Figure 15. Effect of Elevator Feedback on Director/Vehicle Numerator

The resulting lead can be useful in partly offsetting the high frequency lags inherent in the pilot, and reducing the need for pilot lead equalization. However, these are largely accounted for with pitch rate; and considerations of response compatibility and other criteria suggest that the pilot crossover will be low enough to avoid his high frequency limitations anyway.

Elevator feedback has several disadvantages including the following:

- High gains will make the display too sensitive to δ_e motions, and cause the other essential feedbacks to be obscured.
- Undesirable feedback of pilot remnant may result, so any $G_{\delta_e}^{FD}$ needs to contain filtering to smooth the remnant.
- Aircraft trim changes will result in low frequency director errors, avoided by using washout in $G_{\delta_e}^{FD}$.

The fundamental point is that any elevator feedback other than high frequency (above the short period) violates command bar consistency. It is useful at high frequency, to the extent that it indicates aircraft acceleration.

F. SUMMARY OF THE ADVANCED DIRECTOR FEEDBACKS

The requirements of Section II have been used as the basis for the analytical development of an advanced flight director for landing approach which features superior regulation and beam following properties, while being subjectively acceptable to the pilot. The resultant director contains the following feedbacks:

- Beam deviation
- Washed-out pitch attitude
- Beam deviation rate, or washed out altitude rate
- Pitch rate
- Washed-out and filtered elevator (sometimes)

Each of these plays a unique role in satisfying the requirements, although the first three are more essential than the last two.

An overall summary of the effects of different feedbacks and combinations of feedbacks is presented in Table V. The basic and advanced systems are identified. The terms in the "Feedback(s)" column are underlined to indicate that the table entry refers to their contribution. The "Approximate Factors" are intended to apply only to a conventional (jet transport-type) aircraft. "Desired Equalization Location" provides a starting point in determining the appropriate feedback weighting that is most consistent with the requirements, and this is elaborated in the preceding text discussion.

As noted at the outset, the required feedbacks are assumed to be obtained in conventional ways, including the use of complementary filters. This may modify the respective signal waveforms a little, but it should not affect the generality of the results.

Other practical considerations relate to the presence of a glide slope receiver lag, and the effect of the antenna location. The receiver lag introduces a dipole at approximately the lag frequency in the effective director/vehicle transfer function, and it tends to reduce the damping, $\zeta_{\theta}\omega_{\theta}$, of the numerator thereby decreasing the available path mode bandwidth. When the receiver is not at the aircraft c.g., sensed beam deviation will include an $\ell_x\dot{\theta}$ component. For forward locations, this will provide increased path damping; but the effect is slight even at extreme locations.

TABLE V

SUMMARY OF FEEDBACK INFLUENCES ON DIRECTOR/VEHICLE CONTROLLED ELEMENT, FD/δ_e

SYSTEM	FEEDBACK(S)	FUNCTION	NUMERATOR EQUALIZATION	APPROXIMATE FACTORS	DESIRED EQUALIZATION LOCATION	REMARKS
Basic	d	Basic path control allows glide slope capture				Unacceptable alone. $1/T_{h_1}$ must be positive. Display sensitivity set for acceptable low frequency errors.
	d, $\underline{\dot{\theta}}$	Attitude stiffness Path damping	$[\zeta_\theta ; \omega_\theta]$ (may be real)	$\zeta_\theta\omega_\theta \doteq \frac{1}{2T_{\theta_2}}$ $\omega_\theta^2 \doteq \frac{-Z_\alpha K_d}{K_\theta}$	$\omega_p < \omega_\theta < \omega_{sp}$ $\frac{1}{T_{WO}} < \omega_p$	K_d/K_θ small enough to eliminate conditionally stable system. K_d/K_θ large enough for mid-frequency validity. Attitude must be washed out at low frequency.
	d, $\underline{\dot{h}}$	Path damping	$\frac{1}{T_1}$	$\frac{1}{T_1} \doteq \frac{K_d}{K_{\dot{h}}}$	$\frac{1}{T_1} \geq \omega_p$	Minimum phase dip at ω_p. Provide K/s region for crossover. Set acceptable path mode damping. Lacks attitude command bar consistency. Has poor response compatibility.
	d, $\underline{\theta, \dot{h}}$	Path damping Attitude stiffness w_g windproofing	$\frac{1}{T_1}$; $\frac{1}{T_2}$	$\frac{1}{T_1} \doteq \frac{K_d}{K_{\dot{h}}}$ $\frac{1}{T_2} \doteq \frac{-Z_\alpha K_{\dot{h}}}{K_\theta}$	$\frac{1}{T_1} \geq \omega_p$ $\frac{1}{T_2} \doteq \omega_{sp}$ $\frac{1}{T_{\theta_2}} < \frac{1}{T_{WO}} < \omega_{sp}$	Minimum phase dip at ω_p. Provide K/s region for crossover. Set acceptable path mode damping. Attitude washed out at mid-frequency.
	d, $\underline{\theta, \dot{\theta}}$	Attitude stiffness Attitude damping	$\frac{1}{T_E}$	$\frac{1}{T_E} = \frac{K_\theta}{K_{\dot{\theta}}} + \frac{1}{T_{WO}}$	$\frac{1}{T_E} \geq \omega_{sp}$ $\frac{1}{T_{WO}} \geq \omega_p$	Attitude washed out at low frequency. Rate feedback must not make the command bar "busy."
Advanced	d, θ, $\dot{h}$, $\underline{\dot{\theta}}$	Extends region of K/s for crossover	$\frac{1}{T_1}$, $[\zeta_\theta ; \omega_\theta]$	$\frac{1}{T_1} \doteq \frac{K_d}{K_{\dot{h}}}$ $2\zeta_\theta\omega_\theta \doteq \frac{1}{T_{\theta_2}} - \frac{Z_\alpha K_{\dot{h}}}{K_{\dot{\theta}}}$ $\omega_\theta^2 \doteq \frac{-Z_\alpha K_{\dot{h}}}{K_\theta}\left(\frac{1}{T_{W_2}} + \frac{K_\theta}{K_{\dot{\theta}}}\right)$	$\frac{1}{T_1} \geq \omega_p$ $\omega_\theta \doteq \omega_{sp}$ $\frac{1}{T_{\theta_2}} < \frac{1}{T_{WO}} < \omega_{sp}$	Attitude washed out at mid-frequency. Maximum $1/T_1$ limited by mid-frequency phase droop.
	d, θ, $\dot{\theta}$, $\dot{h}$, $\underline{\delta_e}$	Quickens display	Same as above, plus $\frac{1}{T_{\delta_e}}$	Same as above, plus $\frac{1}{T_{\delta_e}} \sim \frac{1}{K_{\delta_e}}$	Same as above, plus $\frac{1}{T_{\delta_e}} > \omega_{sp}$	Only useful at high frequency. Requires washout and high frequency lag. Not required in advanced director. Violates command bar consistency requirement at high frequency.
	d, θ, $\underline{\int d}$	Trim changes, curved beams. w_g, u_g windproofing	Same as d, θ, plus dipole: $\frac{(s + 1/T_{\bar{d}})}{s}$	Same as d, θ, plus $\frac{1}{T_{\bar{d}}} = \frac{K_{\bar{d}}}{K_d}$	Same as d, θ, plus $\frac{1}{T_{\bar{d}}} \doteq \frac{1}{T_{h_1}}$	Violates face validity at low frequency. Must be limited if used. Attitude washed out at low frequency.

SECTION IV

SUMMARY AND IMPLICATIONS

A. OVERALL RESULTS

A comprehensive set of functional requirements, basic principles, and analytical procedures have been presented for specifying and designing flight director/vehicle systems. These permit the designer to select, equalize, and weight the director feedbacks analytically, given the (augmented) vehicle dynamics and a definition of the task. By using these design techniques the final optimization process using actual pilots during simulation and flight test can be planned and accomplished much more expeditiously. Experimental optimization should now become a "fine tuning" procedure, involving overall gain selection and, perhaps, minor changes in the predicted relative weightings.

The basic feedbacks required in a director are beam deviation and washed-out pitch attitude. The addition of beam deviation rate (or its near equivalent, altitude rate) helps provide a K/s-like form for the director/vehicle in the mid-frequency region, improves path damping, and permits more rapid pitch attitude washout. Adding pitch rate helps extend the potential pilot crossover region by offsetting high frequency pilot lags and increasing the gain margin (if the short period is lightly damped).

Although augmenters may improve the system properties, they do not usually have a large effect on the form of the director/vehicle dynamics in the mid-frequency region where pilot crossover will occur. Instead, their principal effect is on fringe areas. For example:

- With a lightly damped short period an increase in pitch rate damping improves the maximum attainable flight director loop bandwidth;
- An autothrottle reduces the speed deviation, improves the speed settling time, and damps the phugoid.

An exception is blended direct lift control which can increase the potential path mode bandwidth by increasing $1/T_{\theta_2}$ and modifying the path numerator.

This would permit higher pilot gain while maintaining the $|\theta/\gamma|$ modal response ratio at an acceptable value.

This report emphasizes longitudinal control, but the procedure and considerations are the same for the lateral axes. The functional requirements are pertinent to lateral and longitudinal landing-approach tasks. With minor changes, the requirements of Section II would also be applicable to other tasks such as curved beam following, flare, and takeoff rotation and climbout.

B. NEW ASPECTS OF THE EVOLVED DESIGN PRINCIPLES

As a paradigm for analytical synthesis of flight director computers, this report contains some new principles and techniques, which arise largely as a result of pilot-centered requirements. These new concepts are summarized below:

- The director synthesis procedure involves the interaction and tradeoff of guidance and control and pilot-centered considerations.
- The effective director/vehicle controlled element should look like a K/s over a broad mid-frequency region.
- The director display should be consistent with status information — low frequency and steady-state bar motions should be beam deviation, the mid-frequency deviations should reflect corresponding vehicle motions, and high frequency (above short period) motions should be attenuated.
- The compatibility of attitude and path motions has an important influence on pilot gain and system crossover frequency. Unfortunately, selection of suitable $|\theta/\gamma|$ ratios at the dominant mode is currently a weak area for both autopilot and flight director design.
- Scanning required to monitor status information will tend to reduce the pilot's gain (Refs. 3 and 5), and this can be avoided by suitably integrating the status information on the display.

C. OTHER IMPLICATIONS FOR DESIGN

The combined requirements and the analytical synthesis procedures lead to other implications for director design that are more or less well known. These are listed below:

- Beam command desensitization is desirable so that the pilot does not have to continuously modify his gain.
- Lags in the director display instrument can reduce the attainable path mode bandwidth, if they are significant in the mid-frequency region.
- The glide slope receiver lag will decrease the attainable path mode bandwidth, as it does with non-director (manual) or autopilot control. Higher quality ILS beams will increase the performance potential of advanced flight control systems by allowing the receiver lag to be decreased.
- Beam integral is needed to achieve good beam following with higher order inputs such as w-gust shears and curved beams. If this is included as a director computer function, the display may be inconsistent for lower order inputs, resulting in standoffs.
- As an alternative to beam integration, the pilot can perform the function based on (non-director) status information. Some compromise is probably the best solution; and this might consist of a selectable mode for curved beams, or a combination of limited integral feedback and pilot integration.

D. FLIGHT DIRECTOR AS A MONITOR

A fundamental pilot-centered consideration is that the pilot will tend to adapt his response so that the pilot-plus-director system has dynamic properties similar to the pilot-plus-raw data system. In effect, in configuring the director/vehicle system the preferred pilot loop closures and equalizations are drawn forward from the pilot and placed in the director computer. On the other hand, for pilot monitoring of (fully automatic) coupled approaches the director output should approximate that of the autopilot.

To simultaneously satisfy these requirements the loop dynamics of the director/vehicle should look like both the pilot/vehicle and the autopilot/vehicle. In practice, the goal would be to make the autopilot and flight director correspond at the dominant modes of the automatic system. The main difference between the closed-loop operation of the pilot and the autopilot would be higher loop gain with the latter.

REFERENCES

1. McRuer, Duane, Henry R. Jex, Warren F. Clement, and Dunstan Graham, A Systems Analysis Theory for Displays in Manual Control, Systems Technology, Inc., Tech. Rept. 163-1, Oct. 1967 (revised June 1968), AD 675983.

2. Clement, Warren F., Henry R. Jex, and Dunstan Graham, "A Manual Control-Display Theory Applied to Instrument Landings of a Jet Transport," IEEE Trans., Vol. MMS-9, No. 4, Dec. 1968, pp. 93-110.

3. Allen, R. W., W. F. Clement, and H. R. Jex, Research on Display Scanning, Sampling, and Reconstruction Using Separate Main and Secondary Tracking Tasks, Systems Technology, Inc., NASA CR-1569, July 1970.

4. Weir, David H., and Richard H. Klein, The Measurement and Analysis of Pilot Scanning and Control Behavior During Simulated Instrument Approaches, Systems Technology, Inc., NASA CR-1535, June 1970.

5. Clement, Warren, and Lee Gregor Hofmann, A Systems Analysis of Manual Control Techniques and Display Arrangements for Instrument Landing Approaches in Helicopters. Vol. I, Speed and Height Regulation, Systems Technology, Inc., JANAIR Rept. 690718, July 1969, AD 700946.

6. McRuer, Duane T., and Henry R. Jex, "A Review of Quasi-Linear Pilot Models," IEEE Trans., Vol HFE-8, No. 3, Sept. 1967, pp. 231-249.

7. McRuer, Duane, Dunstan Graham, Ezra Krendel, and William Reisener, Jr., Human Pilot Dynamics in Compensatory Systems — Theory, Models, and Experiments with Controlled Element and Forcing Function Variations, AFFDL-TR-65-15, July 1965.

8. McRuer, D., and D. H. Weir, "Theory of Manual Vehicular Control," Ergonomics, Vol. 12, No. 4, 1969, pp. 599-633.

9. Melvin, William W., Effects of Wind Shear on Approach with Associate Faults of Approach Couplers and Flight Directors, AIAA Paper 69-796, July 1969.

10. McRuer, D. T., L. G. Hofmann, H. R. Jex, et al, New Approaches to Human-Pilot/Vehicle Dynamic Analysis, AFFDL-TR-67-150, Feb. 1968.

APPENDIX A

VEHICLE EQUATIONS AND TRANSFER FUNCTIONS

THREE DEGREE OF FREEDOM

Equations of Motion* — Body-fixed stability axes, $W_o = 0$.

$$\begin{bmatrix} s - X_u & -X_w & g\cos\Theta_o \\ -Z_u & s - Z_w & -U_o s + g\sin\Theta_o \\ -M_u & -(M_{\dot{w}}s + M_w) & s(s - M_q) \end{bmatrix} \begin{bmatrix} u \\ w \\ \theta \end{bmatrix} = \begin{bmatrix} X_\delta & -X_\eta \\ Z_\delta & -Z_\eta \\ M_\delta & -M_\eta \end{bmatrix} \begin{bmatrix} \delta \\ \\ \eta \end{bmatrix}$$

$$\dot{d} = -w + U_o\theta + \ell_x\dot{\theta}, \text{ at station } \ell_x$$

$$\dot{h} = -w\cos\Theta_o + u\sin\Theta_o + U_o\cos\Theta_o\theta$$

$$a_z = \dot{w} - U_o\dot{\theta} + g\sin\Theta_o\theta - \ell_x\ddot{\theta}, \text{ at station } \ell_x$$

Transfer Function

$$\frac{\theta}{\delta} = \frac{N_\delta^\theta}{\Delta}, \quad \frac{\dot{d}}{\eta} = \frac{sN_\eta^d}{\Delta} = \frac{-N_\eta^w + (U_o + s\ell_x)N_\eta^\theta}{\Delta}, \text{ etc.}$$

Characteristic Function

$$\Delta = (A_\Delta s^4 + B_\Delta s^3 + C_\Delta s^2 + D_\Delta s + E_\Delta)$$

$$A_\Delta = 1$$

$$B_\Delta = -(M_q + Z_w + U_o M_{\dot{w}} + X_u)$$

$$C_\Delta = M_q Z_w - U_o M_w + X_u(M_q + Z_w + U_o M_{\dot{w}}) - X_w Z_u + g M_{\dot{w}}\sin\Theta_o$$

$$D_\Delta = -X_u(Z_w M_q - U_o M_w) - M_u U_o X_w + M_q Z_u X_w + g\cos\Theta_o(M_u + Z_u M_{\dot{w}}) + g\sin\Theta_o(M_w - X_u M_{\dot{w}})$$

$$E_\Delta = g\cos\Theta_o(M_w Z_u - M_u Z_w) + g\sin\Theta_o(M_u X_w - M_w X_u)$$

*The nominal glide slope is $\Theta_o = \gamma_o$.

Beam Deviation Numerators

$$sN_\delta^d = A_\delta^d s^3 + B_\delta^d s^2 + C_\delta^d s + D_\delta^d$$

$$A_\delta^d = -Z_\delta$$

$$B_\delta^d = Z_\delta(U_o M_{\dot{w}} + M_q + X_u) - X_\delta Z_u$$

$$C_\delta^d = U_o[M_{\dot{w}}(X_\delta Z_u - Z_\delta X_u) + (Z_\delta M_w - Z_w M_\delta)] + M_q(Z_u X_\delta - X_u Z_\delta) + gM_\delta \sin \Theta_o$$

$$D_\delta^d = U_o[X_\delta(Z_u M_w - M_u Z_w) - Z_\delta(M_{\dot{w}} X_u - X_w M_u) - M_\delta(X_w Z_u - Z_w X_u)] + g \cos \Theta_o(Z_u M_\delta - M_u Z_\delta) + g \sin \Theta_o(M_u X_\delta - X_u M_\delta)$$

$$sN_\eta^d = A_\eta^d s^3 + B_\eta^d s^2 + C_\eta^d s + D_\eta^d$$

$$A_\eta^d = +Z_\eta$$

$$B_\eta^d = -Z_\eta(U_o M_{\dot{w}} + M_q + X_u) + X_\eta Z_u$$

$$C_\eta^d = U_o[M_{\dot{w}}(Z_\eta X_u - X_\eta Z_u) + (M_\eta Z_w - Z_\eta M_w)] + M_q(X_u Z_\eta - Z_u X_\eta) - gM_\eta \sin \Theta_o$$

$$D_\eta^d = U_o[X_\eta(M_u Z_w - Z_u M_w) + Z_\eta(M_w X_u - X_w M_u) + M_\eta(X_w Z_u - Z_w X_u)] + g \cos \Theta_o(Z_\eta M_u - Z_u M_\eta) + g \sin \Theta_o(X_u M_\eta - M_u X_\eta)$$

Pitch Attitude Numerators

$$N_\delta^\theta = A_\delta^\theta s^2 + B_\delta^\theta s + C_\delta^\theta$$

$$A_\delta^\theta = Z_\delta M_{\dot{w}} + M_\delta$$

$$B_\delta^\theta = X_\delta(M_{\dot{w}} Z_u + M_u) + Z_\delta(M_w - M_{\dot{w}} X_u) - M_\delta(Z_w + X_u)$$

$$C_\delta^\theta = X_\delta(M_w Z_u - M_u Z_w) + Z_\delta(M_u X_w - M_w X_u) + M_\delta(Z_w X_u - X_w Z_u)$$

$$N_\eta^\theta = A_\eta^\theta s^2 + B_\eta^\theta s + C_\eta^\theta$$

$$A_\eta^\theta = -(Z_\eta M_{\dot{w}} + M_\eta)$$

$$B_\eta^\theta = -X_\eta(M_{\dot{w}} Z_u + M_u) - Z_\eta(M_w - M_{\dot{w}} X_u) + M_\eta(Z_w + X_u)$$

$$C_\eta^\theta = -X_\eta(M_w Z_u - M_u Z_w) - Z_\eta(M_u X_w - M_w X_u) - M_\eta(Z_w X_u - X_w Z_u)$$

Vertical Velocity Numerators

$$N_\delta^w = A_\delta^w s^3 + B_\delta^w s^2 + C_\delta^w s + D_\delta^w$$

$$A_\delta^w = Z_\delta$$

$$B_\delta^w = -Z_\delta(M_q + X_u) + U_o M_\delta + X_\delta Z_u$$

$$C_\delta^w = X_u(Z_\delta M_q - U_o M_\delta) - g M_\delta \sin \Theta_o + X_\delta(M_u U_o - Z_u M_q)$$

$$D_\delta^w = g(Z_\delta M_u - M_\delta Z_u)\cos \Theta_o + g \sin \Theta_o(M_\delta X_u - X_\delta M_u)$$

$$N_\eta^w = A_\eta^w s^3 + B_\eta^w s^2 + C_\eta^w s + D_\eta^w$$

$$A_\eta^w = -Z_\eta$$

$$B_\eta^w = Z_\eta(M_q + X_u) - U_o M_\eta - X_\eta Z_u$$

$$C_\eta^w = X_u(U_o M_\eta - Z_\eta M_q) + M_\eta g \sin \Theta_o - X_\eta(M_u U_o - Z_u M_q)$$

$$D_\eta^w = g \cos \Theta_o(M_\eta Z_u - Z_\eta M_u) + g \sin \Theta_o(X_\eta M_u - M_\eta X_u)$$

Forward Velocity Numerators

$$N_\delta^u = A_u s^3 + B_u s^2 + C_u s + D_u$$

$$A_u = X_\delta(1 - Z_{\dot{w}})$$

$$B_u = -X_\delta[M_q(1 - Z_{\dot{w}}) + Z_w + M_{\dot{\alpha}}] + Z_\delta X_w$$

$$C_u = X_\delta(M_q Z_w - M_\alpha) - Z_\delta(g M_{\dot{w}} \cos \Theta_o + M_q X_w) + M_\delta[X_\alpha - (g \cos \Theta_o)(1 - Z_{\dot{w}})] + g X_\delta M_{\dot{w}} \sin \Theta_o$$

$$D_u = g(Z_w M_\delta - M_w Z_\delta)\cos \Theta_o + g(X_\delta M_w - M_\delta X_w)\sin \Theta_o$$

$$N_\eta^u = A_\eta^u s^3 + B_\eta^u s^2 + C_\eta^u s + D_\eta^u$$

$$A_\eta^u = -X_\eta$$

$$B_\eta^u = X_\eta(M_q + M_{\dot{\alpha}} + Z_w) - X_w Z_\eta$$

$$C_\eta^u = M_q(X_w Z_\eta - Z_w X_\eta) + U_o(X_\eta M_w - X_w M_\eta) + g \cos \Theta_o(Z_\eta M_{\dot{w}} + M_\eta) - g \sin \Theta_o X_\eta M_{\dot{w}}$$

$$D_\eta^u = g \sin \Theta_o(X_w M_\eta - X_\eta M_w) + g \cos \Theta_o(Z_\eta M_w - Z_w M_\eta)$$

Coupling Numerators

$$sN^{d\ \theta}_{\eta\ \delta} = A^{d\ \theta}_{\eta\ \delta}s + B^{d\ \theta}_{\eta\ \delta}$$

$$A^{d\ \theta}_{\eta\ \delta} = Z_\eta M_\delta - M_\eta Z_\delta$$

$$B^{d\ \theta}_{\eta\ \delta} = -X_u(Z_\eta M_\delta - M_\eta Z_\delta) + Z_u(X_\eta M_\delta - M_\eta X_\delta) - M_u(X_\eta Z_\delta - Z_\eta X_\delta)$$

$$N^{u\ w}_{\delta\ \eta} = A^{u\ w}_{\delta\ \eta}s^2 + B^{u\ w}_{\delta\ \eta}s + C^{u\ w}_{\delta\ \eta}$$

$$A^{u\ w}_{\delta\ \eta} = X_\eta Z_\delta - Z_\eta X_\delta$$

$$B^{u\ w}_{\delta\ \eta} = M_q(Z_\eta X_\delta - X_\eta Z_\delta) + U_o(X_\eta M_\delta - M_\eta X_\delta)$$

$$C^{u\ w}_{\delta\ \eta} = g\cos\Theta_o(M_\delta Z_\eta - Z_\delta M_\eta) + g\sin\Theta_o(M_\eta X_\delta - M_\delta X_\eta)$$

$$N^{u\ \theta}_{\delta\ \eta} = A^{u\ \theta}_{\delta\ \eta}s + B^{u\ \theta}_{\delta\ \eta}$$

$$A^{u\ \theta}_{\delta\ \eta} = M_{\dot{w}}(X_\eta Z_\delta - Z_\eta X_\delta) + X_\eta M_\delta - M_\eta X_\delta$$

$$B^{u\ \theta}_{\delta\ \eta} = X_\eta(Z_\delta M_w - M_\delta Z_w) + Z_\eta(M_w X_\delta - M_\delta X_w) + M_\eta(X_\delta Z_w - X_w Z_\delta)$$

$$s^2 N^{h\ d}_{\delta_e\eta} = A^{u\ \dot{d}}_{\delta_e\eta}s^2 + B^{u\ \dot{d}}_{\delta_e\eta}s + C^{u\ \dot{d}}_{\delta_e\eta}$$

$$A^{u\ \dot{d}}_{\delta_e\eta} = [X_\delta Z_\eta - X_\eta Z_\delta]\sin\Theta_o$$

$$B^{u\ \dot{d}}_{\delta_e\eta} = (M_q + M_{\dot{u}})(X_\eta Z_\delta - X_\delta Z_\eta)\sin\Theta_o$$

$$C^{u\ \dot{d}}_{\delta_e\eta} = g\cos\Theta_o\sin\Theta_o(Z_\delta M_\eta - Z_\eta M_\delta) + g\sin\Theta_o^2(X_\eta M_\delta - X_\delta M_\eta)$$
$$+ U_o\sin\Theta_o[M_w(X_\eta Z_\delta - Z_\eta X_\delta) + Z_w(X_\delta M_\eta - X_\eta M_\delta) + X_w(Z_\eta M_\delta - M_\eta Z_\delta)]$$

$$N^{\dot{d}\ \theta}_{\eta\ \delta} = -N^{w\ \theta}_{\eta\ \delta} = N^{\theta\ w}_{\eta\ \delta}$$

$$sN^{d\ u}_{\eta\ \delta} = s\left[-N^{u\ w}_{\delta\ \eta} + U_o N^{u\ \theta}_{\delta\ \eta}\right]$$

SHORT PERIOD EQUATIONS

Equations of Motion

$$\begin{bmatrix} s(s-Z_w) & Z_\alpha \\ s(M_{\dot{w}}s+M_w) & s^2-(M_q+M_{\dot{\alpha}})s-M_\alpha \end{bmatrix} \begin{bmatrix} d \\ \theta \end{bmatrix} = \begin{bmatrix} Z_\delta & -Z_\eta \\ M_\delta & -M_\eta \end{bmatrix} \begin{bmatrix} \delta \\ \eta \end{bmatrix}$$

Characteristic Function

$$\Delta = s^2\left[s^2-(M_q+M_{\dot{\alpha}}+Z_w)s-(M_\alpha-Z_wM_q)\right]$$

Transfer Function Numerators

$$N_\delta^d = -Z_\delta\left[s^2-(M_q+M_{\dot{\alpha}})s-\left(M_\alpha-\frac{M_\delta}{Z_\delta}Z_\alpha\right)\right] = A_\delta^d s^2+B_\delta^d s+C_\delta^d$$

$$N_\eta^d = Z_\eta\left[s^2-(M_q+M_{\dot{\alpha}})s-\left(M_\alpha-\frac{M_\eta}{Z_\eta}Z_\alpha\right)\right] = A_\eta^d s^2+B_\eta^d s+C_\eta^d$$

$$N_\delta^\theta = s\left[(M_\delta+Z_\delta M_{\dot{w}})s-(M_\delta Z_w-Z_\delta M_w)\right] = s\left[A_\delta^\theta s+B_\delta^\theta\right]$$

$$N_\eta^\theta = -s\left[(M_\eta+Z_\eta M_{\dot{w}})s-(M_\eta Z_w-Z_\eta M_w)\right] = -s\left[A_\eta^\theta s+B_\eta^\theta\right]$$

Coupling Numerators

$$N_{\eta\ \delta}^{d\ \theta} = M_\delta Z_\eta - Z_\delta M_\eta$$

APPENDIX B

STEADY-STATE BEAM FOLLOWING AND GUST REGULATION

The function of the flight director is to maintain the aircraft on the glide slope when the command bar error is nulled by the pilot. Whether the flight director can produce zero beam deviations in steady-state (as $t \rightarrow \infty$) depends on the nature of the command and disturbance inputs, as well as the equalization of the feedback signals.

This appendix develops the analytical expressions for steady-state longitudinal beam error in the presence of arbitrary beam commands and gusts. The resulting control implications are examined for the following specific inputs:

- Power series beam command
- Dual angle beam command
- Step and shear (ramp) vertical gusts
- Step and shear (ramp) horizontal gusts

Although the limiting steady-state cases are examined, landing approach involves only a short time duration. Hence, the practical concern is with the errors at the end of the landing approach.

BEAM FOLLOWING

With the basic attitude plus beam deviation system the beam error* equation for an arbitrary beam command, $h_c(s)$, is

$$h_e(s) = \left[\frac{\Delta + G_{FD}^{\delta_e}\left(G_\theta^{FD} N_{\delta_e}^{\theta} + G_{h-h_c}^{FD} N_{\delta_e}^{h}\right)}{\Delta + G_{FD}^{\delta_e}\left(G_\theta^{FD} N_{\delta_e}^{\theta} + G_h^{FD} N_{\delta_e}^{h}\right)}\right] h_c(s) \qquad \text{(B-1)}$$

*Beam error can be described by d_e or h_e in the context of beam command inputs.

The equalization terms, G, are defined in Fig. 7 of the main text, and the airframe transfer function polynomials are given in Appendix A. Since an $\dot{h}$ feedback is not included,

$$G^{FD}_{h-h_c} = G^{FD}_{h} - G^{FD}_{h_c} = 0 \tag{B-2}$$

Deleting this term in Eq. B-1 and taking the limit as $s \rightarrow 0$ gives the following steady-state result:

$$h_e\Big]_{ss} = \lim_{s \rightarrow 0} s\left[\frac{s\left(G^{\delta_e}_{FD} G^{FD}_{\theta} C^{\theta}_{\delta_e} + E_{\Delta}\right)}{G^{\delta_e}_{FD} G^{FD}_{h} D^{h}_{\delta_e}}\right] h_c(s) \tag{B-3}$$

This applies for the general case where throttle setting is not changed and airspeed is allowed to vary.

If the pilot holds constant airspeed, Eq. B-3 reduces to the following 2 degree of freedom expression (when Z_{δ_e} is neglected):

$$h_e\Big]_{ss} = \lim_{s \rightarrow 0} s\left[\frac{sG^{FD}_{\theta}}{U_o G^{FD}_{h}}\right] h_c(s) \tag{B-4}$$

If the commanded path is given by a power series in time, i.e.,

$$h_c(t) = h_1 + h_2 t + h_3 t^2 + \cdots h_n t^{n-1} \tag{B-5}$$

This has the Laplace transform,

$$h_c(s) = \frac{h_1}{s} + \frac{h_2}{s^2} + \frac{2h_3}{s^3} + \cdots \frac{(n-1)!h_n}{s^n} \tag{B-6}$$

Then the steady-state error in the three degree of freedom case is obtained by substituting in Eq. B-3, i.e.,

$$h_e\Big]_{ss} = \lim_{s \to 0} \left[\frac{s\left(G_{FD}^{\delta_e} G_\theta^{FD} C_{\delta_e}^{\theta} + E_\Delta\right)}{G_{FD}^{\delta_e} G_h^{FD} D_{\delta_e}^{h}} \right] \frac{(n-1)!h_n}{s^{n-1}} \qquad \text{(B-7)}$$

The corresponding two degree of freedom result is

$$h_e\Big]_{ss} = \lim_{s \to 0} \left[\frac{sG_\theta^{FD}}{U_o G_h^{FD}} \right] \frac{(n-1)!h_n}{s^{n-1}} \qquad \text{(B-8)}$$

To satisfy the requirements of Section II, Eqs. B-7 and B-8 show that the numerator must contain a free s^n if the system is to have zero steady-state beam error for an n^{th} order power series command. In the case of a step, h_1/s, the system will have zero steady-state beam error when the equalizations, G, are gains only.

The higher order terms in the power series, Eq. B-5, lead to the requirement for equalizations other than gain (e.g., additional feedbacks). From the sketch it is apparent that a system which is stabilized on the first segment of a dual angle glide path must follow a ramp function in h without steady-state error if it is to successfully transition from paths 1 to 2. So a free s^2 is needed in the bracketed portion of Eqs. B-7 or B-8. This is obtained in different ways depending on which equation is used.

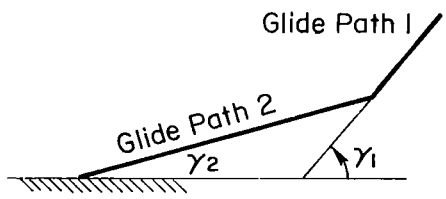

If the pilot changes throttle setting to hold airspeed constant (Eq. B-8), G_θ^{FD} must either

- Contain a free s via washed out pitch attitude,

$$G_\theta^{FD} = \frac{K_\theta s}{s + 1/T_{w_o}} \quad , \text{ or}$$

- Have an integral term in the denominator, for example, via a parallel integrator on the beam signal

$$G_h^{FD} = \frac{K_{\overline{d}}}{s}$$

This latter alternative has the disadvantage that integrators accumulate small errors which could cause the flight director to be off center when the aircraft is stabilized on the beam and the beam error is zero. This would give the pilot a director command contradictory to his status information.

In the three degree of freedom case (airspeed not held constant), the ramp input into Eq. B-7 could be handled by washing out attitude and letting the pilot retrim the elevator (i.e., $G_{FD}^{\delta e} \doteq K_1 + K_2/j\omega$).

Higher order inputs, for example, curved path commands, would require at least a free s^3 in Eqs. B-7 and B-8. This would demand beam integration feedback in addition to pilot elevator trim and washed out θ.

GENERALIZED GUST REGULATION

The flight director must permit pilot control to compensate for wind (or gust) disturbances. At very low frequency (steady state) this implies maintaining the aircraft on the beam in the presence of step gusts, shears, and vehicle trim changes. Satisfactory steady-state performance is again achieved by suitable equalization of the feedback signals to the director.

The beam deviation response to a generalized external wind velocity disturbance, $\eta(s)$, is shown in the block diagram of Fig. B-1.

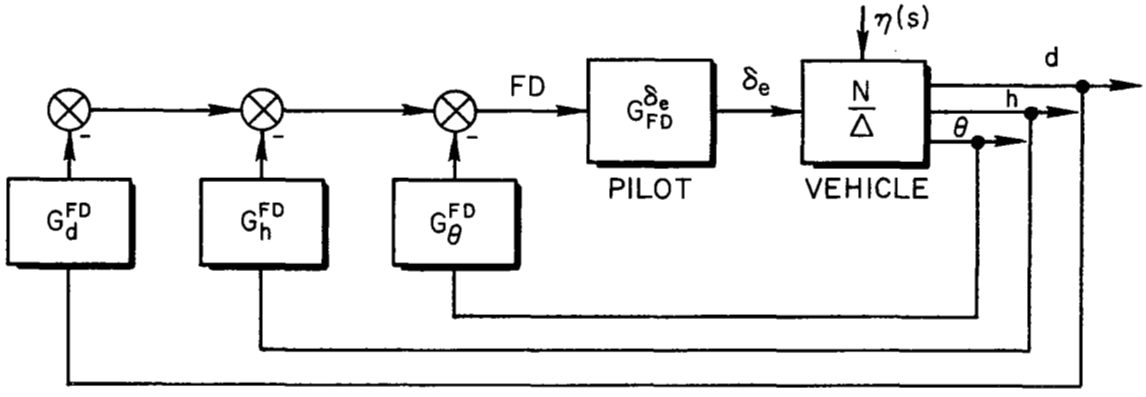

Figure B-1. Flight Director Feedbacks with Gust Inputs

The beam deviation transfer function to a generalized gust, $\eta(s)$, is:

$$d_e = \left[\frac{N_\eta^d + G_{FD}^{\delta_e}\left(G_\theta^{FD} N_\eta^{d\ \theta}_{\delta_e} + G_h^{FD} N_\eta^{d\ h}_{\delta_e}\right)}{\Delta + G_{FD}^{\delta_e}\left(G_\theta^{FD} N_{\delta_e}^{\theta} + G_d^{FD} N_{\delta_e}^{d} + G_h^{FD} N_{\delta_e}^{h}\right)} \right] \eta(s) \qquad \text{(B-9)}$$

A distinction between d and h is now made to properly account for steady state wind effects. This difference produces the coupling numerator, $N_\eta^{d\ h}_{\delta_e}$. The disturbance, η, can result from a vertical, or horizontal, wind, and either can have a constant velocity component, i.e., $\eta(s) = \eta_1/s + \cdots$. Because of the stability axis system used, a horizontal (head or tail) wind contains both u_g and w_g components, along the x and z axes, respectively. To cause no residual beam error for the constant velocity component requires that

$$d_e\Big]_{ss} = \lim_{s \to 0} s\left[\ \right] \frac{\eta_1}{s} = 0 \qquad \text{(B-10)}$$

where the term in brackets is defined by Eq. B-9. This condition is satisfied when there is at least one free s in the numerator of the term in brackets. Other expressions for the response to a generalized gust are given in Table B-I at the end of this Appendix.

VERTICAL GUST, w_g

When only attitude equalization is used, the three degree of freedom steady-state expression for beam deviation due to a generalized $w_g(s)$ is

$$d_e\Big]_{ss} = \lim_{s \to 0} s\left[\frac{N_{w_g}^{\dot{d}} + G_{FD}^{\delta_e} G_\theta^{FD} N_{\delta_e w_g}^{\theta\ \dot{d}}}{s\Delta + G_{FD}^{\delta_e}\left(G_\theta^{FD} N_{\delta_e}^{\theta} + G_{\dot{d}}^{FD} N_{\delta_e}^{\dot{d}}\right)} \right] w_g(s) \qquad \text{(B-11)}$$

And this reduces to

$$d_e\Big]_{ss} = \lim_{s \to 0} s\left[\frac{D_{w_g}^{d} + G_{FD}^{\delta_e} G_\theta^{FD} B_{w_g \delta_e}^{d\ \theta}}{G_{FD}^{\delta_e} G_\theta^{FD} D_{\delta_e}^{d}} \right] w_g(s) \qquad \text{(B-12)}$$

The terms $D^{d}_{w_g}$, $B^{d\ \theta}_{w_g \delta_e}$ and $D^{d}_{\delta_e}$ are the lowest order terms in the numerator expressions when $s \rightarrow 0$. Using the values from Appendix A, the complete three degree of freedom steady-state expression for beam error to a w-gust is

$$d_e\Big]_{ss} = \lim_{s \rightarrow 0} s \left\{ \frac{\begin{array}{r}(M_u Z_w - M_w Z_u)(g \cos \Theta_o + G^{\delta_e}_{FD} G^{FD}_{\theta} X_\delta) + (X_u M_w - M_u X_w)(g \sin \Theta_o + G^{\delta_e}_{FD} G^{FD}_{\theta} Z_\delta) \\ + G^{\delta_e}_{FD} G^{FD}_{\theta} M_\delta (Z_u X_w - Z_w X_u)\end{array}}{G^{\delta_e}_{FD} G^{FD}_{d} \left[\begin{array}{r}(Z_\delta M_u - M_\delta Z_u)(U_o X_w - g \cos \Theta_o) + (X_u M_\delta - M_u X_\delta)(U_o Z_w - g \sin \Theta_o) \\ + U_o M_w (Z_u X_\delta - X_u Z_\delta)\end{array} \right]} \right\} w_g(s) \qquad \text{(B-13)}$$

Expressions for this and other vehicle motions resulting from a w-gust are given in Table B-I.

The equalization requirements are determined by the fact that the expression in brackets in Eq. B-13 must contain numerator free s terms of the same order as the input, $w_g(s)$. Because the numerator within the brackets is a constant as $s \rightarrow 0$, the free s terms needed to cancel those in $w_g(s)$ must come from the denominator within the brackets. One free s can be obtained by the pilot, $G^{\delta_e}_{FD}$, retrimming the elevator, i.e., acting as a parallel integrator in the elevator channel and having G^{FD}_{θ} include a washout of the pitch attitude. An alternative is to include a $K_{\dot{d}}/s$ component in the G^{FD}_{d} control path. A similar argument applies for step trim changes resulting in Z_o and M_o, lift and pitching, accelerations applied to the vehicle.

Shear (ramp) inputs, on the other hand, require the same equalization as a step, plus a $K_{\dot{d}}/s$ component in the G^{FD}_{d} control path. If beam integral equalization is not acceptable, the flight director will not show an existing steady state beam error caused by a w_g shear even if the pilot holds the director bar centered. Hence the guidance and control requirements conflict with the pilot-centered requirements in this case. Ways around this conflict include the following:

- Provide a separate director mode for shears which includes beam integration. This will also satisfy the (second order) curved beam requirement, discussed above.

- Include beam integration feedback in the flight director and limit its authority.
- Provide other (beam error) status information to the pilot so that he can essentially double integrate the beam error, avoiding beam integration in the director computer.

Each of these solutions can be found in current practice.

As an alternate technique, the pilot or an automatic controller can attempt to maintain a constant airspeed by throttle changes. In this case the steady-state beam deviation can be derived from the two degree of freedom approximation of Appendix A to give

$$d_e\Big]_{ss} = \lim_{s \to 0} s\left[\frac{-Z_w s(M_{\dot{\alpha}} + M_q) + G_{FD}^{\delta_e} G_\theta^{FD}(M_\delta Z_w - M_w Z_\delta)}{G_{FD}^{\delta_e} G_d^{FD}(M_\delta Z_\alpha - M_\alpha Z_\delta)}\right] w_g(s) \qquad \text{(B-14)}$$

Again, $w_g(s)$ is generalized. With washed-out attitude feedback, the drift from the beam caused by a step w-gust is reduced to zero by virtue of the aircraft's weather-cocking tendency. The pilot will have to make a change in power setting, however, because

$$\theta\Big]_{ss} = \lim_{s \to 0} s\left(\frac{1}{U_o}\right) w_g(s) \qquad \text{(B-15)}$$

For a w-gust shear input, the pitch angle and power setting must be continuously changed (as a ramp) in order to hold the command bar centered. In this case, with washed-out pitch attitude, the aircraft will remain at a constant steady-state beam error equal to:

$$d_e\Big]_{ss} = \frac{K_\theta T_{w_o}}{U_o K_h}(w_{g_2}) \text{ , ft} \qquad \text{(B-16)}$$

where w_{g_2} is the magnitude of the shear in ft/sec^2. Note that the beam error is reduced as the attitude is washed out faster. Beam integral

feedback would also be helpful in this two degree of freedom case, because it would provide the additional free s in the numerator necessary to produce zero steady-state error.

HORIZONTAL GUST, u_g

Substituting $u_g(s)$ for $\eta(s)$ in the general d/η expression, Eq. B-9, yields

$$\frac{d_e}{u_g}(s) = \left[\frac{N^d_{u_g} + G^{\delta_e}_{FD}\left(G^{FD}_{\theta} N^{\theta}_{\delta_e} N^{d}_{u_g} + G^{FD}_{h} N^{d}_{u_g} N^{h}_{\delta_e}\right)}{\Delta + G^{\delta_e}_{FD}\left(G^{FD}_{\theta} N^{\theta}_{\delta_e} + G^{FD}_{d} N^{d}_{\delta_e} + G^{FD}_{h} N^{h}_{\delta_e}\right)}\right] \tag{B-17}$$

In the three degree of freedom case (when airspeed is allowed to vary) the constant terms of $sN^d_{u_g}$ and $sN^{\theta}_{\delta_e} N^{d}_{u_g}$ are zero. The steady-state expression, found by letting $s \to 0$, is therefore:

$$d_e\Big]_{ss} = \lim_{s \to 0} s\left[\frac{sC^d_{u_g} + G^{\delta_e}_{FD}\left(sG^{FD}_{\theta} A^{d\ \theta}_{u_g \delta_e} + G^{FD}_{h} C^{u\ \dot{d}}_{\delta_e u_g}\right)}{G^{\delta_e}_{FD}\left(G^{FD}_{d} D^{d}_{\delta_e} + G^{FD}_{h} D^{h}_{\delta_e}\right)}\right] u_g(s) \tag{B-18}$$

where $C^d_{u_g}$, $A^{d\ \theta}_{u_g \delta_e}$, $C^{u\ d}_{\delta_e u_g}$, and $D^d_{\delta_e}$ are the lowest order term in the respective numerators. When $G^{FD}_h = 0$, Eq. B-18 reduces to

$$d_e\Big]_{ss} = \lim_{s \to 0} s^2\left[\frac{U_o(M_u Z_w - Z_u M_w) - g\, M_u \sin \Theta_o + G^{\delta_e}_{FD} G^{FD}_{\theta}(Z_u M_\delta - M_u Z_\delta)}{G^{\delta_e}_{FD} G^{FD}_{d} D^{d}_{\delta_e}}\right] u_g(s) \tag{B-19}$$

Note that a free s occurs in this expression. Step u-gusts produce zero steady-state beam error without any feedback equalization or pilot retrimming. Other steady-state expressions are given in Table B-I.

A u-gust shear requires washed-out attitude and pilot retrim. The initial response is reduced in magnitude as $M_u Z_w - Z_u M_w$ is made smaller, and is, in fact, one argument for neutral static stability of the airframe alone. In the limit the u-gust shear causes a steady-state airspeed change which will normally be countered by the pilot with the thrust correction

necessary to bring the aircraft back "on airspeed." The trim power change is simply $\Delta T = m(du_g/dt)$. As pointed out in Ref. 9 this trim change may be a critical one, especially for decreasing tailwind shears that stop near the ground, leaving the pilot with insufficient power.

These steady state considerations indicate that the most troublesome disturbance inputs are wind shears. The worst of these is a shear normal to the flight path, for it causes a low frequency beam error even with attitude washout and the pilot retrimming elevator and power. The need to wash out attitude feedback as rapidly as possible also tends to conflict with the path damping requirements of Section II.

TABLE B-I. SUMMARY OF STEADY-STATE GUST RESPONSES

System Definition

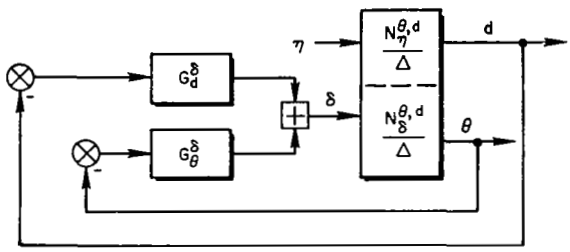

Response for Generalized Gust, η(s)

$$d]_{ss} = \lim_{s\to 0} s\left[\frac{N_\eta^{\dot{d}} + G_\theta^\delta N_\delta^\theta \dot{d}_\eta}{\Delta s + G_\theta^\delta s N_\delta^\theta + G_d^\delta N_\delta^{\dot{d}}}\right]\eta(s) = \lim_{s\to 0} s\left[\frac{D_\eta^d - G_\alpha^\delta B_\delta^\alpha \dot{w}_\eta}{G_d^\delta D_\delta^d}\right] r(s)$$

$$\theta]_{ss} = \lim_{s\to 0} s\left[\frac{N_\eta^\theta \dot{d}_\delta}{N_\delta^{\dot{d}}}\right]\eta(s) = \lim_{s\to 0} s\left[\frac{-N_\eta^\theta \dot{w}_\delta}{N_\delta^{\dot{d}}}\right]\eta(s) = \lim_{s\to 0} s\left[\frac{B_\delta^\theta \dot{w}_\eta}{D_\delta^d}\right]\eta(s)$$

$$w]_{ss} = \lim_{s\to 0} s\left[\frac{N_\eta^w \dot{d}_\delta}{N_\delta^{\dot{d}}}\right]\eta(s) = \lim_{s\to 0} s\left[\frac{U_o N_\eta^w \theta_\delta}{N_\delta^{\dot{d}}}\right]\eta(s) = \lim_{s\to 0} s\left[\frac{U_o B_\delta^\theta w_\eta}{D_\delta^d}\right]\eta(s)$$

$$u]_{ss} = \lim_{s\to 0} s\left[\frac{N_\eta^u \dot{d}_\delta}{N_\delta^{\dot{d}}}\right]\eta(s) = \lim_{s\to 0} s\left[\frac{-N_\eta^u w_\delta + U_o N_\eta^u \theta_\delta}{N_\delta^{\dot{d}}}\right]\eta(s) = \lim_{s\to 0} s\left[\frac{-B_\eta^u w_\delta + U_o B_\delta^\alpha u_\eta}{D_\delta^d}\right]\eta(s)$$

Response for Vertical Gust, $w_g(s)$

$$d]_{ss} = \lim_{s\to 0} s\left\{\frac{(M_u Z_w - M_w Z_u)(g\cos\Theta_o + G_\theta^\delta X_\delta) + (X_u M_w - M_u X_w)(g\sin\Theta_o + G_\theta^\delta Z_\delta) + G_\theta^\delta M_\delta(Z_u X_w - Z_w X_u)}{G_d^\delta\left[g\cos\Theta_o(M_\delta Z_u - Z_\delta M_u) + g\sin\Theta_o(X_\delta M_u - M_\delta X_u)\right] + U_o\left[X_\delta(M_w Z_u - M_u Z_w) + Z_\delta(M_u X_w - M_w X_u) + M_\delta(Z_w X_u - X_w Z_u)\right]}\right\} w_g'(s)$$

$$\theta]_{ss} = \lim_{s\to 0} s\left[\frac{X_u(Z_w M_\delta - Z_\delta M_w) + Z_u(X_\delta M_w - X_w M_\delta) + M_u(Z_\delta X_w - X_\delta Z_w)}{D_\delta^d}\right] w_g'(s)$$

$$w]_{ss} = \lim_{s\to 0} s\; w_g'(s)$$

$$u]_{ss} = \lim_{s\to 0} s\left[\frac{g\cos\Theta_o(Z_w M_\delta - Z_\delta M_w) - g\sin\Theta_o(X_w M_\delta - X_\delta M_w)}{D_\delta^d}\right] w_g'(s)$$

For Horizontal Gust, $u_g(s)$

$$d]_{ss} = \lim_{s\to 0} s^2\left[\frac{\left[U_o(M_u Z_w - Z_u M_w) - g M_u \sin\Theta_o\right] + \left[G_\theta^\delta(Z_u M_\delta - M_u Z_\delta)\right]}{G_d^\delta D_\delta^d}\right] u_g'(s)$$

$$\theta]_{ss} = \lim_{s\to 0} \frac{s^2(M_u Z_\delta - Z_u M_\delta)}{D_\delta^d}\, u_g'(s)$$

$$w]_{ss} = \lim_{s\to 0} \frac{s^2 U_o(M_u Z_\delta - Z_u M_\delta)}{D_\delta^d}\, u_g'(s)$$

$$u]_{ss} = \lim_{s\to 0} s\; u_g'(s)$$

APPENDIX C

EXAMPLE APPLICATION OF FLIGHT DIRECTOR DESIGN PRINCIPLES TO THE DC-8 AIRCRAFT

This appendix presents a numerical illustration of the flight director synthesis techniques developed in Section III. The longitudinal dynamics of an unaugmented DC-8 aircraft trimmed for the landing approach configuration (from Ref. 4) are used to represent the vehicle. The airframe parameters and stability derivatives are given in Table C-I. Numerical values for the transfer function numerators and denominators are given in Table C-II, based on the definitions in Appendix A.

TABLE C-I

DC-8 PARAMETERS FOR LANDING APPROACH CONFIGURATION

GEOMETRY AND INERTIA		LONGITUDINAL STABILITY AXES	
h (ft)	0	X_u (1/sec)	−0.0372
M (−)	0.204	X_w (1/sec)	0.136
V_{T_o} (ft/sec)	228.	X_{δ_e} (ft/sec^2/rad)	0
γ_o (deg)	0	X_{δ_T} (ft/sec^2/%)	0.106
q (lb/ft^2)	61.8	Z_u (1/sec)	−0.283
S (ft^2)	2758.	Z_w (1/sec)	−0.750
b (ft)	142.4	$Z_{\dot{w}}$ (−)	0
c (ft)	22.16	Z_{δ_e} (ft/sec^2/rad)	−9.25
W (lb)	180,000.	Z_{δ_T} (ft/sec^2/%)	−0.00097
m (slugs)	5,580.	M_u (1/sec-ft)	0
ℓ_x (ft)	60.	M_w (1/sec-ft)	−0.00461
I_y (slug-ft^2)	3.8×10^6	$M_{\dot{w}}$ (1/ft)	−0.00085
I_{xz} (slug-ft^2)	0	M_{δ_e} (1/sec^2)	−0.923
X_{CG} (% c)	25.2	M_{δ_T} (1/sec^2/%)	0
δf_o (deg)	50	M_α (1/sec^2)	−1.05
α_o (deg)	0.62	$M_{\dot{\alpha}}$ (1/sec)	−0.1936

TABLE C-II

LONGITUDINAL STABILITY AXIS TRANSFER FUNCTIONS
FOR THE DC-8 IN THE LANDING APPROACH CONFIGURATION

$$\Delta = [0.0865 \; ; \; 0.166][0.627 \; ; \; 1.23]^{*}$$

$$N_{\delta_e}^{\theta} = -0.915(0.101)(0.646)$$

$$N_{\delta_e}^{u} = -1.258(-4.12)(4.03)$$

$$N_{\delta_e}^{w} = -9.25(23.3)[0.090 \; ; \; 0.198]$$

$$N_{\delta_e}^{\dot{h}} = 9.25(-3.63)(0.0352)(4.42)$$

$$N_{\delta_e}^{a_z'} = 45.66(0)(0.035)[0.192 \; ; \; 1.81]$$

$$N_{\delta_T}^{\theta} = 0$$

$$N_{\delta_T}^{u} = 0.106(-0.0009)[0.636 \; ; \; 1.22]$$

$$N_{\delta_T}^{w} = -0.00097(31.1)(0)(0.59)$$

$$N_{\delta_T}^{\dot{h}} = -0.00097[0.38 \; ; \; 1.02](31.1)$$

$$N_{\delta_e\delta_T}^{\theta \; w} = 0.0009(31.1)$$

$$N_{\delta_e\delta_T}^{\theta \; u} = -0.097(0.709)$$

$$N_{\delta_e\delta_T}^{w \; u} = -0.98(-0.0013)(23.3)$$

$$N_{\delta_e\delta_T}^{\theta \; \dot{h}} = -0.0009(31.1)$$

$$N_{\delta_e\delta_T}^{w \; \dot{h}} = -0.203(31.1)$$

$$N_{\delta_e\delta_T}^{u \; \dot{h}} = -0.98(-3.63)(4.41)$$

$$N_{w_g}^{\dot{h}} = -0.75(0.871)[0.011 \; ; \; 0.254]$$

$$N_{w_g}^{\theta} = 0.004(-0.0087)(0.0378)$$

$$N_{w_g}^{u} = -0.136(0)[0.407 \; ; \; 0.975]$$

$$N_{w_g}^{\dot{h} \; \theta}{}_{\delta_e} = 0.649(0.092)$$

---

*To simplify the notation, $A[s^2 + 2\zeta\omega s + \omega^2]$ is written $A[\zeta \; ; \; \omega]$ and $A(s + a)$ is written $A(a)$.

FEEDBACKS AND EQUALIZATION

Ideal feedbacks containing no significant lags or nonlinearities are assumed to be available to the flight director computer. These can normally be obtained (to a good approximation) with suitable complementary filtering. The feedbacks include:

- Beam angle, γ
- Pitch altitude, θ
- Pitch rate, $\dot{\theta}$
- Instantaneous vertical velocity, $\dot{h}$

Range desensitization converts the beam angle, γ, into a displacement from the beam. In turn, this can be approximated by the perturbation altitude, h.

This example is sufficiently similar to the generic development in Section III that the feedbacks and equalization form evolved there can be applied directly. The resulting feedback functions are:

$$G_\theta^{FD} = \frac{K_\theta s}{s + \frac{1}{T_{WO}}} + K_{\dot{\theta}} s = \frac{K_{\dot{\theta}} s \left(s + \frac{1}{T_{WO}} + \frac{K_\theta}{K_{\dot{\theta}}} \right)}{\left(s + \frac{1}{T_{WO}} \right)}$$

$$G_h^{FD} = K_h + K_{\dot{h}} s = K_{\dot{h}} \left(s + \frac{K_h}{K_{\dot{h}}} \right)$$

First cut values of the gains and washout time constant, T_{WO}, can be selected <u>a priori</u> using the considerations noted in Table V. Specializing these considerations to the vehicle dynamics from Table C-II results in Table C-III, which also gives the first-cut equalization values and associated rationale.

TABLE C-III

SELECTED EQUALIZATION VALUES

EQUALIZATION	EXPRESSION	DESIRED LOCATION AND VEHICLE VALUE	SELECTED EQUALIZATION	REMARKS
Pitch Washout	$\frac{1}{T_{WO}}$	$< \omega_{sp} = 1.23$ $> \frac{1}{T_{\theta 2}} = 0.65$	0.7	Washout less than ω_{sp} to provide attitude stability but greater than $1/T_{\theta_2}$ for windproofing and to maintain altitude bandwidth.
Pitch Attitude	$\frac{1}{T_{WO}} + \frac{K_\theta}{K_{\dot{\theta}}}$	$\geq \omega_{sp} = 1.23$	1.7	Pitch attitude lead set to implement short-period damping and extend the region of K/s by having the resulting ω_θ zeros cancel the ω_{sp} poles.
Altitude	$\frac{K_h}{K_{\dot{h}}}$	$\doteq \omega_p = 0.167$	0.2	Greater than ω_p to avoid a "busy" display and the low frequency closed-loop d/d_c amplitude droop, yet maintain mid-frequency phase margin.

VEHICLE/DIRECTOR TRANSFER FUNCTION

The overall director/vehicle transfer function is

$$\frac{FD}{\delta_e} = \frac{N_{\delta_e}^{FD}}{\Delta} = \frac{G_\theta^{FD} N_{\delta_e}^{\theta} + G_h^{FD} N_{\delta_e}^{h}}{\Delta}$$

The behavior of the numerator as a function of the gain ratio, $K_{\dot{h}}/K_{\dot{\theta}}$, can be evaluated analytically by letting

$$\left[1 + \frac{G_h^{FD} N_{\delta_e}^{h}}{G_\theta^{FD} N_{\delta_e}^{\theta}}\right] = \left[1 + G(s)\right] = 0$$

Numerically, the numerator ratio is:

$$G(s) = \frac{G_h^{FD} N_{\delta_e}^h}{G_\theta^{FD} N_{\delta_e}^\theta} = \frac{K_h^\cdot}{K_{\dot\theta}^\cdot} \frac{9.23(s+0.2)(s+0.042)(s-3.6)(s+4.4)(s+0.7)}{-.915s^2(s+1.7)(s+0.101)(s+0.646)}$$

Figure C-1 is a system survey of this transfer function, consisting of jω-Bode and Bode root locus plots on the right and a conventional root locus plot on the left. The heavy lines are the σ-Bode which show the variation of closed-loop numerator's real roots with gain, $K_h^\cdot/K_{\dot\theta}^\cdot$. The dotted line along the Bode asymptote is the locus of the complex pair ω_θ.

The numerator roots are determined by the gain $K_h^\cdot/K_{\dot\theta}^\cdot$. Selecting a +0.011 rad/ft places the complex pair of roots, ω_θ, near the vehicle short-period frequency to cancel ω_{sp} and extend the K/s region. The complete flight director numerator is then

$$N_{\delta_e}^{FD} = \frac{\left(K_{\dot\theta}^\cdot M_{\delta_e} - K_h^\cdot Z_{\delta_e}\right)\left(s+\frac{1}{T_{h_1}'}\right)\left(s+\frac{1}{T_1}\right)\left(s+\frac{1}{T_{WO}'}\right)\left[s^2+2\zeta_\theta\omega_\theta s+\omega_\theta^2\right]}{s^2\left(s+\frac{1}{T_{WO}}\right)}$$

$$= \frac{(K_{\dot\theta}^\cdot M_{\delta_e} - K_h^\cdot Z_{\delta_e})(s+0.042)(s+0.23)(s+0.76)[s^2+2(0.59)(1.27)s+(1.27)^2]}{s^2(s+0.7)}$$

This is combined with the vehicle characteristic equation, Δ, to give the open-loop director/vehicle transfer function.

The absolute gain values for the effective controlled element are determined when the display scale is established. For example, if a ratio of director bar to pitch (horizon) bar deflection is unity, the director computer gains are the following:

$$K_{\dot\theta}^\cdot = -1.0$$

$$K_\theta = -1.0$$

$$K_h^\cdot = -0.0110 \text{ rad/ft/sec}$$

$$K_h = -0.0022 \text{ rad/ft}$$

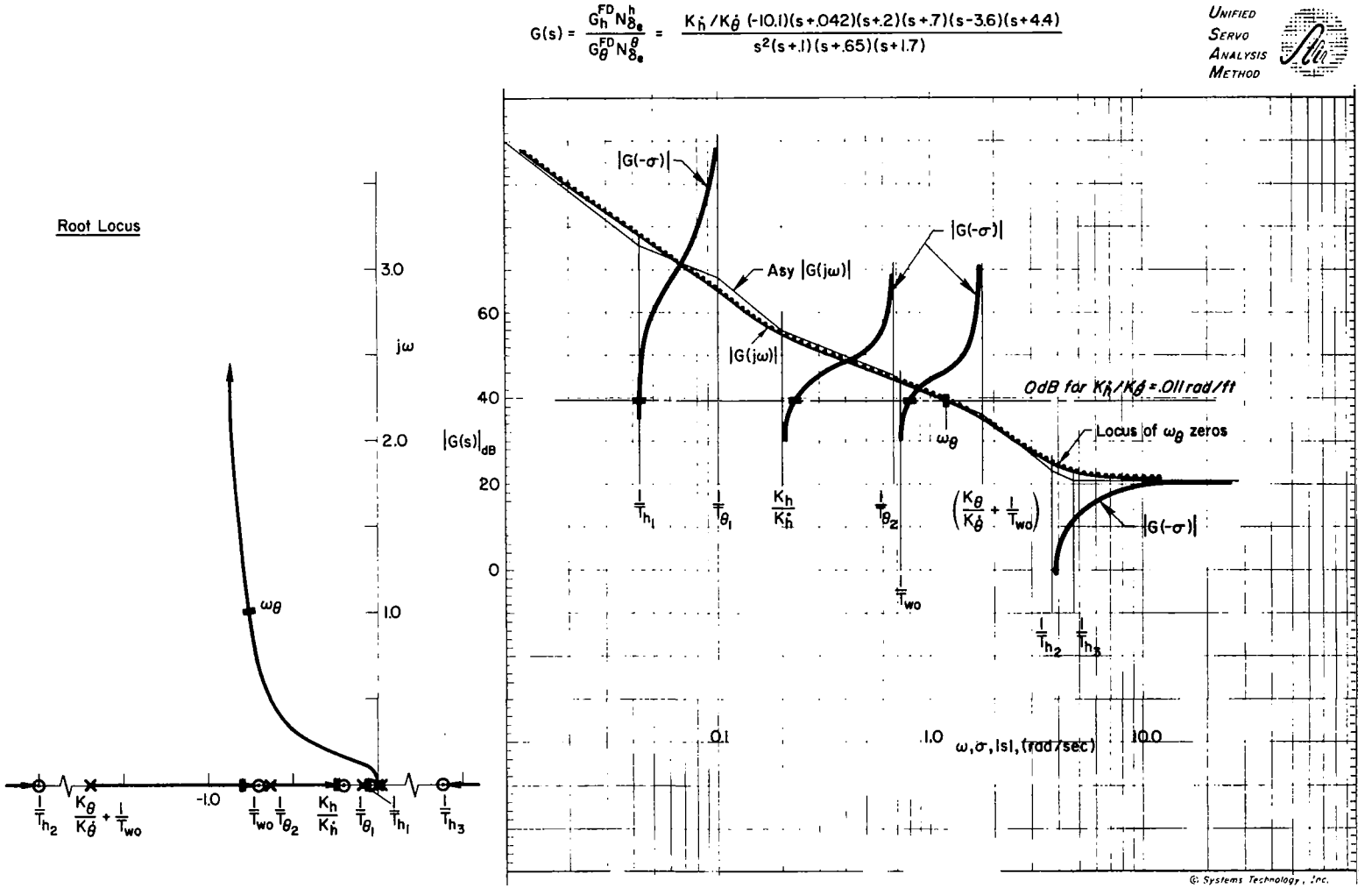

Figure C-1. Flight Director Numerator Survey

PILOT LOOP CLOSURE CONSIDERATIONS

The open-loop director/vehicle, FD/δ_e, system survey is given in Fig. C-2. The equalization terms ($1/T_1$ and ω_θ) do provide the desired K/s-like amplitude ratio over a large frequency region where the pilot should close the loop (the potential crossover region). The wind-proofing and command bar consistency requirements are implicit in the selection of the feedbacks, as discussed in Section III. The actual equalization terms (transfer function zeros) are compared with the approximate characteristic ratios in Table C-IV.

TABLE C-IV

COMPARISON OF APPROXIMATE AND EXACT EQUALIZATION ZEROS

EQUALIZATION TERM	CHARACTERISTIC RATIO APPROXIMATION	CALCULATED VALUE
$\frac{1}{T_1}$	$\frac{K_h}{K_{\dot{h}}} = 0.20$	0.23
ω_θ	$\sqrt{-Z_\alpha \frac{K_{\dot{h}}}{K_{\dot{\theta}}}\left(\frac{1}{T_{WO}} + \frac{K_\theta}{K_{\dot{\theta}}}\right)} = \sqrt{(1.89)(1.7)} = 1.78$	1.27

In closing the loop, the pilot will introduce a time delay, and perhaps some offsetting high frequency lead. This will modify the open-loop system response properties as shown for an assumed pilot time delay, τ, of 0.4 sec by the dashed phase curve in Fig. C-2. This gives the "maximum possible crossover" line which intersects the amplitude ratio plot at about 4 rad/sec. A more realistic "potential crossover region" is also sketched in Fig. C-2, and this is felt to be more typical of what can be expected in a longitudinal director control task on the basis of available models and data. The actual crossover will vary depending on the pilot gain selected to satisfy the guidance and control requirements (see Section II) for particular inputs while at the same time maintaining an acceptable level of vehicle motions (pitch attitude, load factor, etc.).

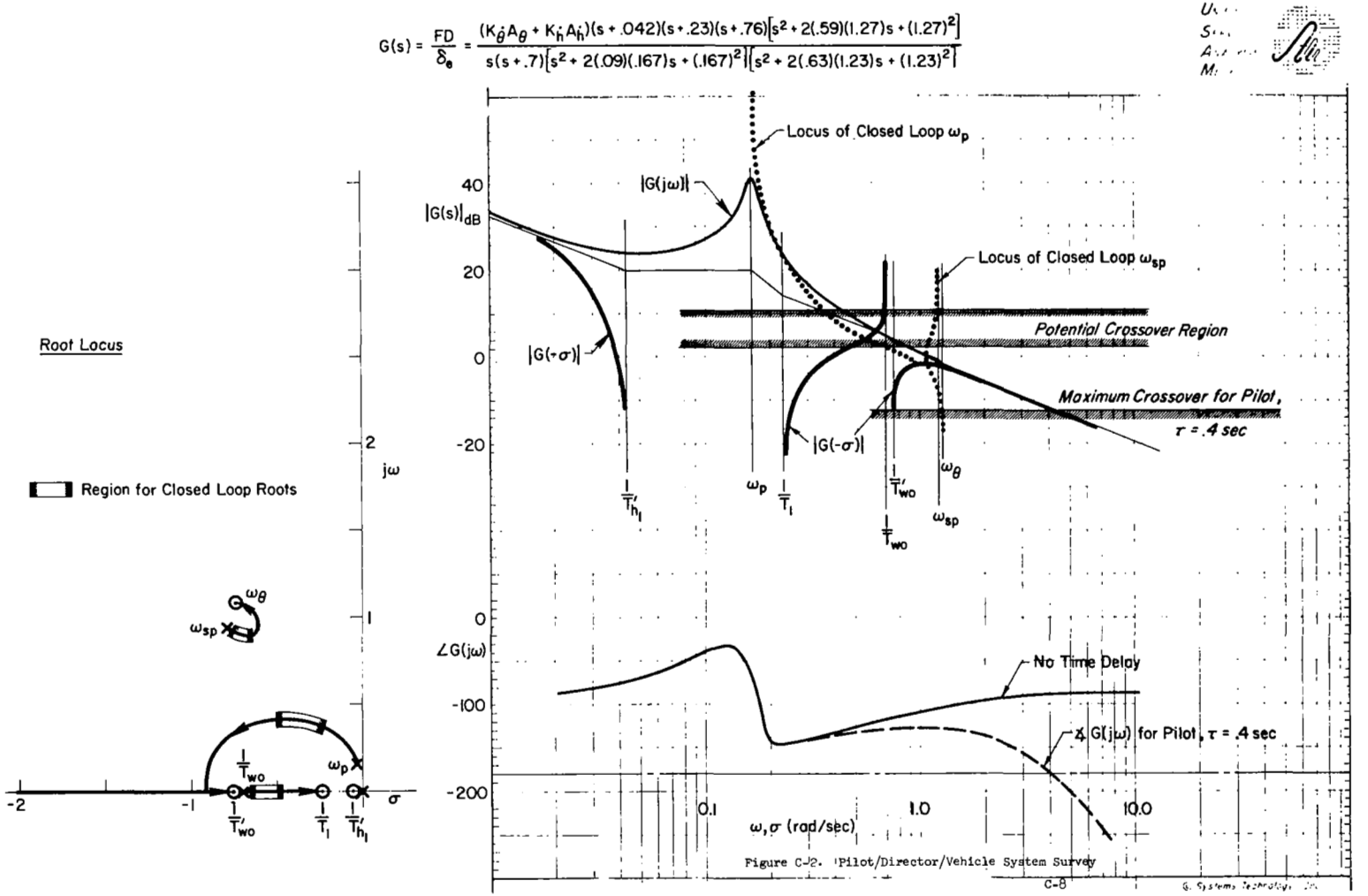

Figure C-2. Pilot/Director/Vehicle System Survey

His gain will vary for different levels of system input (beam bends, turbulence) due to threshold effects. Hence, a key objective is to provide a broad range of K/s-like dynamics so that the nature (mode shape) of the system response is insensitive to variations in pilot gain, whatever the cause.

For large discrete inputs such as an initial beam (step) offset, the pilot's response will differ from that for continuous random inputs. He will tend to operate so that the system responds more rapidly yet with less overshoot (Ref. 10) than the describing function would predict. In the limit, a skilled pilot performing a practiced maneuver may approach a time optimal response, consisting of one well-timed and sized elevator pulse in the case of K/s director/vehicle dynamics. When discrete inputs are not dominant, but are mixed with random inputs in a relatively unpredictable way, then the describing function models are appropriate.

For director control of transport aircraft in landing approach, a primary consideration in estimating pilot gain is the frequency and damping of the resulting closed-loop modes. The pilot will be sensitive to the pitch attitude and altitude rate motions which result from efforts to minimize beam error, and the modal response ratios will vary directly with pilot gain or control effort.

The system of Fig. C-2 presents relatively good vehicle characteristics. With lower short-period damping the potential crossover frequency will have to be reduced in order to stay below any peak in the amplitude ratio. In that case more attitude rate feedback will be necessary. In the opposite sense if the phugoid had had better damping it would not be necessary to use as much $K_{\dot{h}}$ gain, i.e., $1/T_1$ could be increased. These effects are reflected in the modal response ratios, along with the effect of varying pilot gain.

Preferred values for the closed-loop modes can be illustrated with the loci of modal response ratios plotted in Fig. C-3 for the DC-8 example. The loci of modal response ratios plotted are:

- $|\theta/\gamma|$, pitch attitude to path angle; equal to unity
- $|a_z/\theta|$, normal acceleration at the pilot relative to pitch attitude; equal to 0.1g per degree

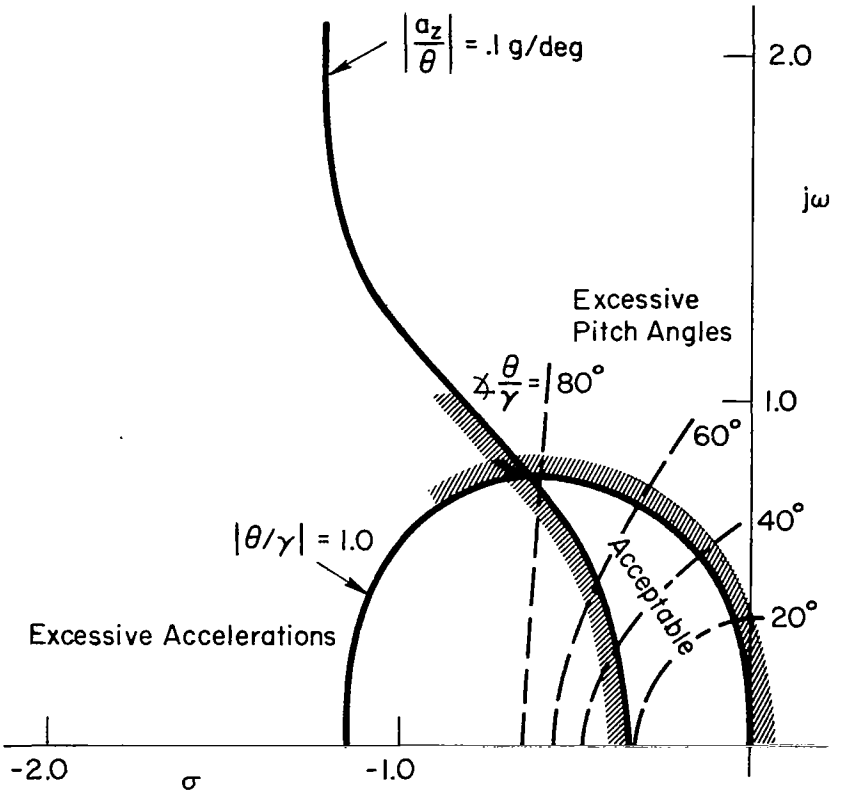

Figure C-3. Modal Response Ratio Boundaries for the DC-8 Example

The chosen criterion values are hypothetical and serve only to illustrate the analysis. The plotted loci were obtained by evaluating the appropriate open-loop numerator ratios at various values* of s, and then plotting the frequency and damping associated with a given amplitude ratio (e.g., $|\theta/\gamma| = 1.0$). The resulting loci form boundaries for excessive pitch attitude and normal acceleration. Superimposing the example boundaries in Fig. C-3 onto the root locus portion of Fig. C-2 indicates the allowable gain region for the closed-loop modes. A crossover frequency of 0.6 rad/sec or less keeps the path mode accelerations due to attitude

*The values of s represent possible values for the dominant mode which would result from pilot closure of the flight director/vehicle control loop in Fig. C-2.

changes less than 0.1g/deg, and the attitude to flight path angle change near unity at short-period frequencies. In other words, the roots on the complex locus in Fig. C-2 lie within the example "acceptable" region in Fig. C-3.

The loop gain associated with a 0.6 rad/sec crossover frequency would be $K_p(K_{\dot\theta}^{\cdot}A_\theta + K_{\dot h}^{\cdot}A_{\dot h}^{\cdot}) = 0.5$. Using the example gains based on $K_{\dot\theta}^{\cdot} = -1.0$ results in $K_p = 0.62$. The closed-loop characteristic equation for this gain is

$$\Delta' = \frac{(s+0.639)(s+0.034)[0.699\ ;\ 0.437][0.624\ ;\ 1.191]}{s(s+0.7)}$$

Another view of the closed-loop motion harmony for this example can be obtained from the beam deviation and pitch angle responses to beam commands. These are given by*

$$\left.\frac{h}{h_c}\right]_{FD\rightarrow\delta_e} = \frac{K_p K_h N_{\delta_e}^{h}}{s\Delta'}$$

$$= \frac{-0.013(s+0.7)(s+0.042)(s-3.6)(s+4.4)}{(s+0.639)(s+0.034)[0.699\ ;\ 0.437][0.624\ ;\ 1.191]}$$

$$\left.\frac{\theta}{h_c}\right]_{FD\rightarrow\delta_e} = \frac{K_p K_h N_{\delta_e}^{\theta}}{\Delta'}$$

$$= \frac{0.071(s+0.7)(s)(s+0.101)(s+0.646)}{(s+0.639)(s+0.034)[0.699\ ;\ 0.437][0.624\ ;\ 1.191]}, \text{ deg/ft}$$

The frequency response plots for a 0.6 rad/sec crossover are shown in Fig. C-4. The beam deviation response is flat out to the dominant mode

*These transfer function forms assume that the $\dot h$ term is obtained by a rate of descent feedback as opposed to an ideal forward loop beam differentiation.

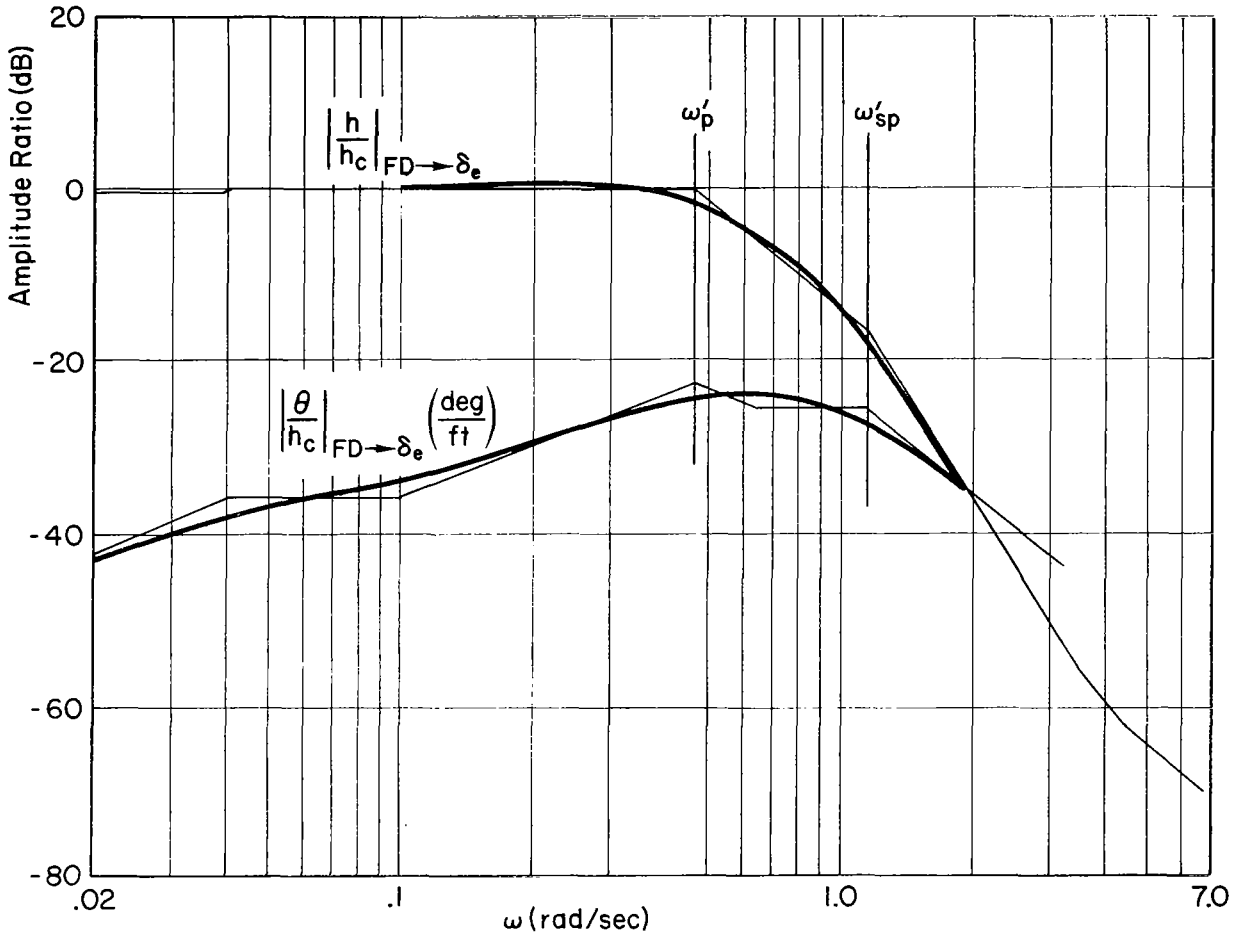

Figure C-4. Closed-Loop Attitude and Beam Deviation Response to Beam Commands for Example Crossover

and then rolls off sharply. The dominant response will be well damped. The attitude response peaks up near the path mode and then rolls off sharply, indicating little attitude overshoot to a beam command. The mode shapes are illustrated in Fig. C-5 by the time responses to a 10 ft beam deviation offset.* The maximum pitch angle excursion is

*This step is assumed to be imbedded in a background of random inputs so that the describing function model is appropriate.

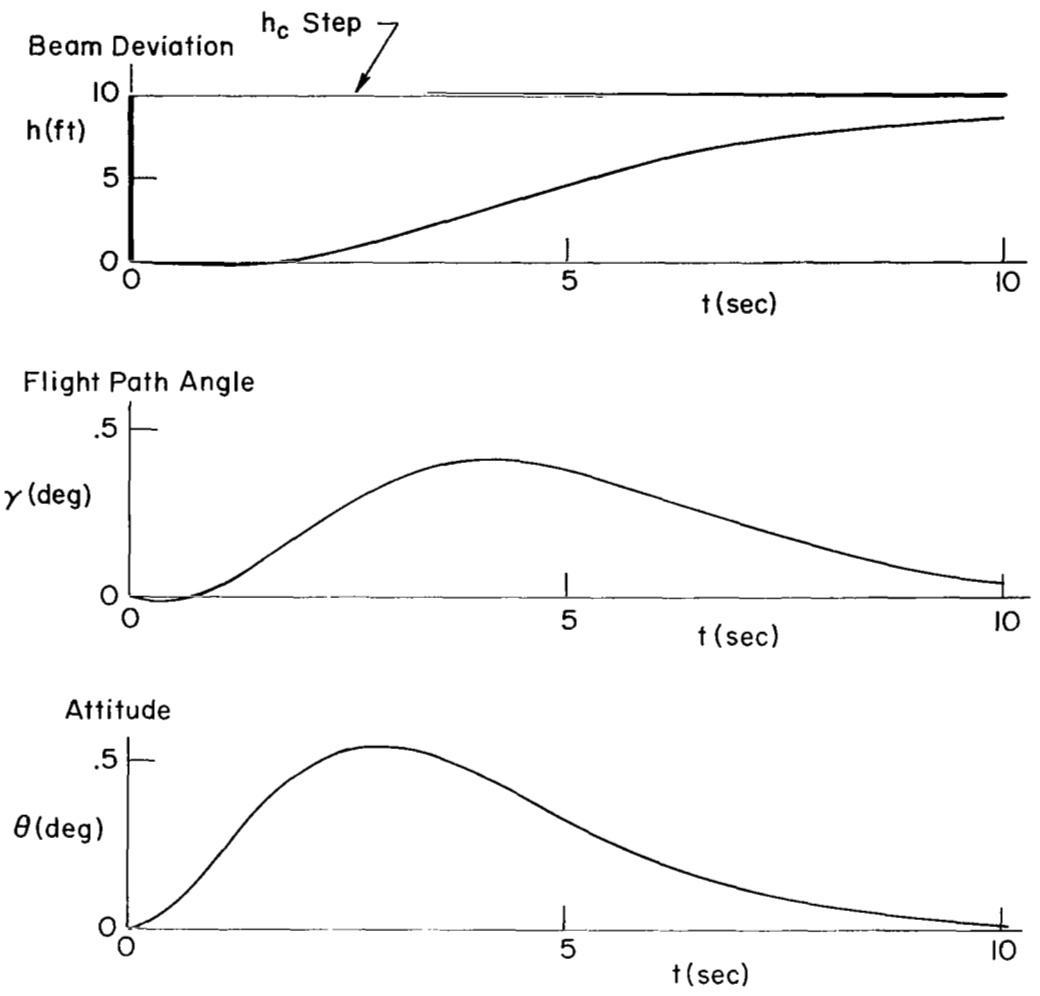

Figure C-5. Beam Deviation and Attitude Time Responses to a 10 Ft Beam Command

is just slightly greater than that of the flight path angle. The beam deviation rise time is relatively slow but this will be quickened as the crossover frequency in Fig. C-2 is increased. The shape (overshoot, etc.) will be similar throughout the K/s region.

Modal response ratios are useful in assessing the closed-loop system properties. Table C-V summarizes the more important ratios at both closed-loop modes for the 0.6 rad/sec crossover example. The θ/γ and a_z/θ ratios at the closed-loop phugoid are within boundaries on Fig. C-3. The θ/h ratio can be used to express the attitude overshoot to a beam command at a

TABLE C-V

MODAL RESPONSE RATIOS FOR EXAMPLE PILOT CLOSURE

MODAL RESPONSE RATIO	CLOSED-LOOP PHUGOID [0.70 ; 0.44]	CLOSED-LOOP SHORT PERIOD [0.62 ; 1.2]
$\frac{\theta}{\gamma}$ (deg/deg)	0.65 ∠ 47°	1.15 ∠ 90°
$\frac{\theta}{h}$ (deg/ft)	0.06 ∠ 162°	0.32 ∠ 225°
$\frac{u}{\theta}$ (ft/sec/deg)	1.75 ∠ 19°	0.45 ∠ −40°
$\frac{a_z}{\theta}$ (g/deg)	0.075 ∠ 275°	0.09 ∠ 200°

given mode by multiyplying the θ/h ratio by the h/h_c response at the same mode yielding the θ/h_c response. This differs from Fig. C-4 in that it includes the damping ratio effect. The small u/θ ratio at short period indicates that the vehicle holds speed well and may not require an autothrottle. At the path mode the speed changes will present little problem to the pilot.

In summary, these modal response considerations include estimation of pilot gain and closed-loop system properties based, at least partially, on what the pilot will consider to be an acceptable repertoire of system responses. This is somewhat different from the usual situation in which the analyst is attempting to estimate pilot gain and system stability margins largely on the basis of predicted path mode error.

APPENDIX D

TYPICAL DIRECTOR INDICATOR DISPLAYS

This appendix contains photographic examples of modern flight director indicators evolved by four manufacturers; Bendix, Collins, Lear, and Sperry. They each contain the same status information but somewhat different flight director command indications, warning flags, and annunciator lights.

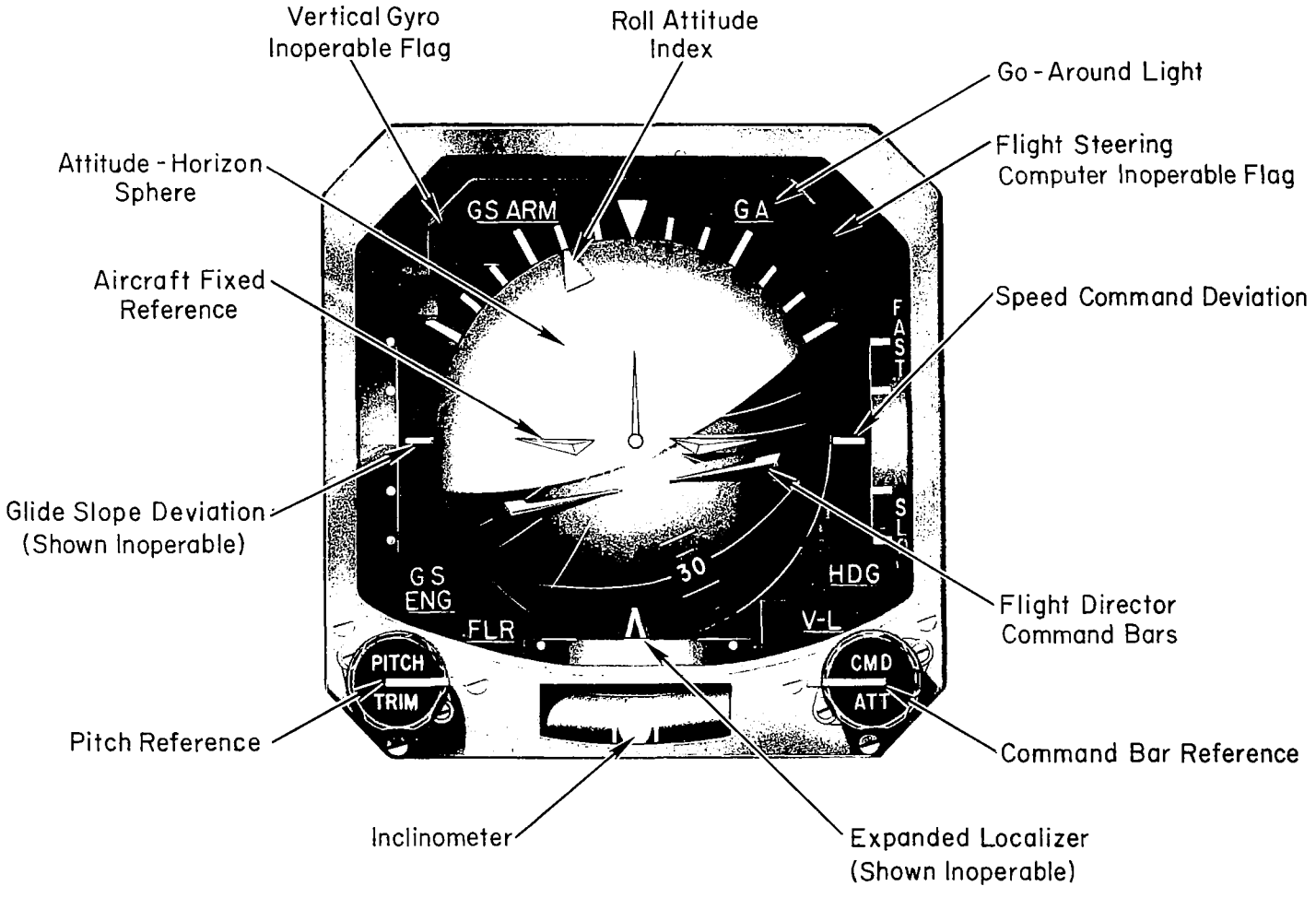

Figure D-1. Bendix FD-60 Horizon and Director Indicator

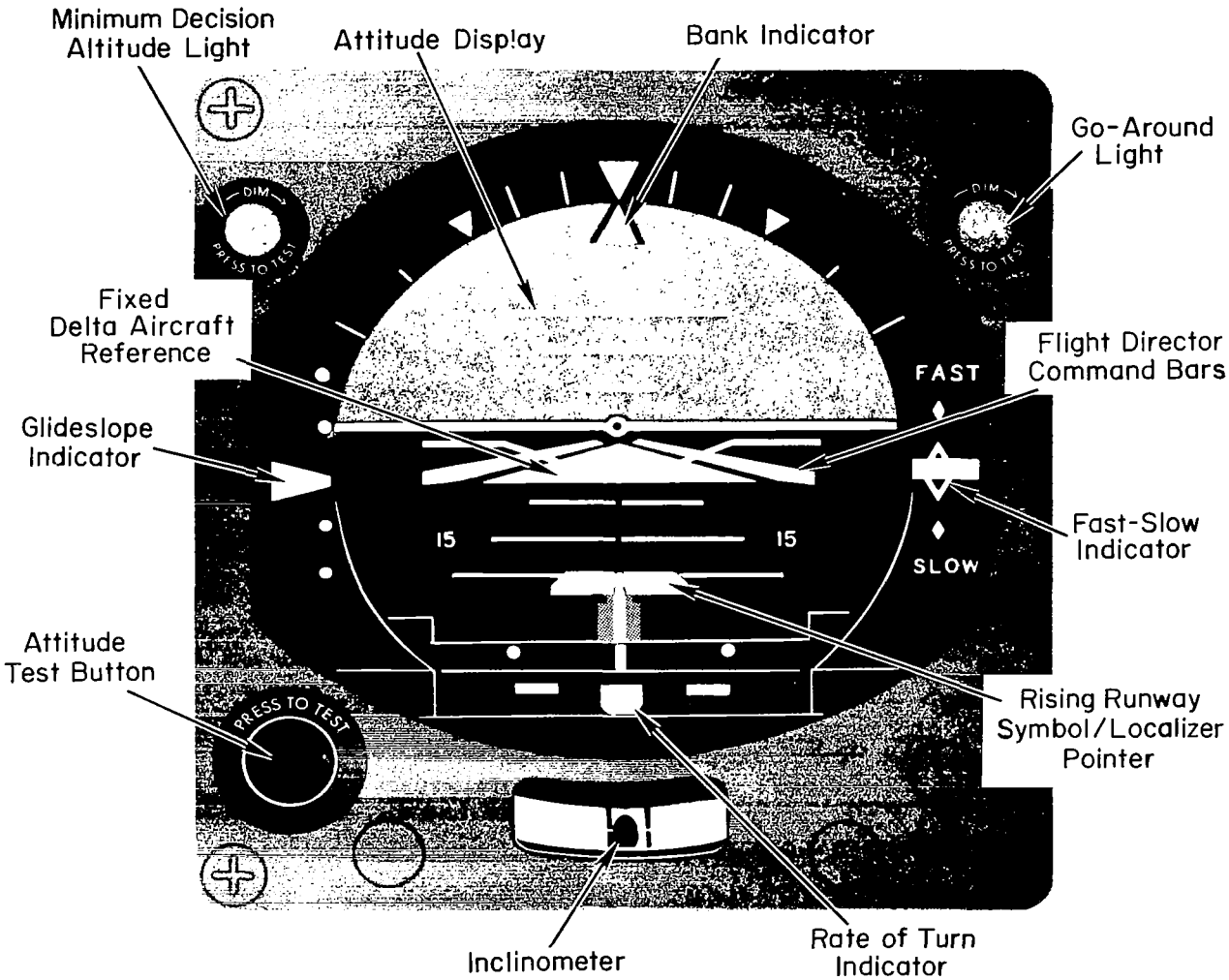

Figure D-2. Collins FD-109 Flight Director Indicator

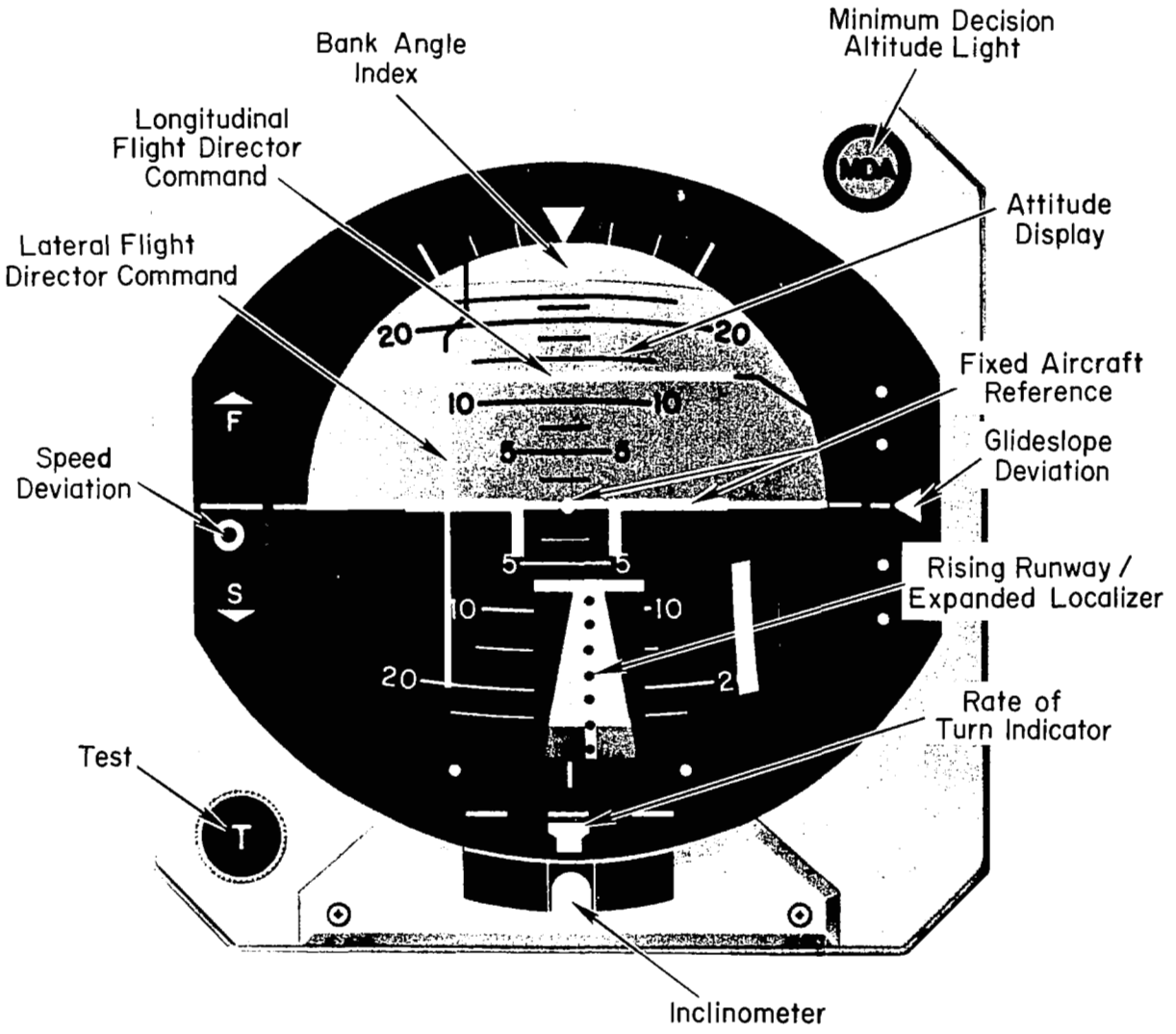

Figure D-3. Lear Model 4058AC Two Axis Attitude Director Indicator

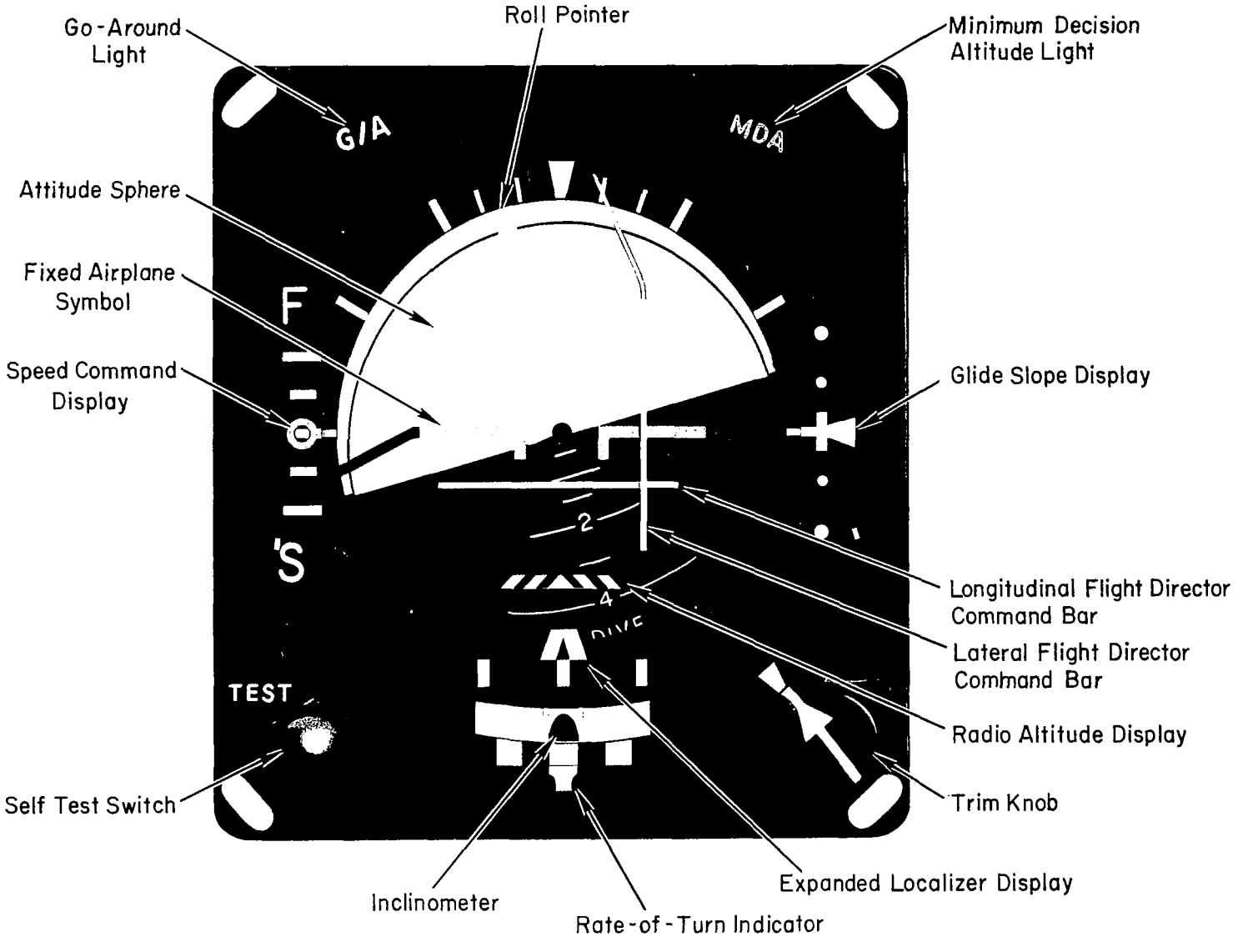

Figure D-4. Sperry HZ-6B Attitude Director Indicator